

REPORT DOCUMENTATION PAGE			Form Approved OMB NO. 0704-0188		
<p>The public reporting burden for this collection of information is estimated to average 1 hour per response, including the time for reviewing instructions, searching existing data sources, gathering and maintaining the data needed, and completing and reviewing the collection of information. Send comments regarding this burden estimate or any other aspect of this collection of information, including suggestions for reducing this burden, to Washington Headquarters Services, Directorate for Information Operations and Reports, 1215 Jefferson Davis Highway, Suite 1204, Arlington VA, 22202-4302. Respondents should be aware that notwithstanding any other provision of law, no person shall be subject to any penalty for failing to comply with a collection of information if it does not display a currently valid OMB control number. PLEASE DO NOT RETURN YOUR FORM TO THE ABOVE ADDRESS.</p>					
1. REPORT DATE (DD-MM-YYYY) 30-11-2007		2. REPORT TYPE Final Report		3. DATES COVERED (From - To) 1-Sep-2006 - 31-Aug-2007	
4. TITLE AND SUBTITLE Dual Channel Transmission for Coexistence of Wireless Networks			5a. CONTRACT NUMBER W911NF-06-1-0415		
			5b. GRANT NUMBER		
			5c. PROGRAM ELEMENT NUMBER 611102		
6. AUTHORS Xiangqian Liu			5d. PROJECT NUMBER		
			5e. TASK NUMBER		
			5f. WORK UNIT NUMBER		
7. PERFORMING ORGANIZATION NAMES AND ADDRESSES University of Louisville Research Foundation, Inc. 2301 S. Third Street Louisville, KY 40208 -			8. PERFORMING ORGANIZATION REPORT NUMBER		
9. SPONSORING/MONITORING AGENCY NAME(S) AND ADDRESS(ES) U.S. Army Research Office P.O. Box 12211 Research Triangle Park, NC 27709-2211			10. SPONSOR/MONITOR'S ACRONYM(S) ARO		
			11. SPONSOR/MONITOR'S REPORT NUMBER(S) 51908-C1.1		
12. DISTRIBUTION AVAILABILITY STATEMENT Approved for Public Release; Distribution Unlimited					
13. SUPPLEMENTARY NOTES The views, opinions and/or findings contained in this report are those of the author(s) and should not be construed as an official Department of the Army position, policy or decision, unless so designated by other documentation.					
14. ABSTRACT With the upcoming pervasive deployment of wireless networks and devices on the unlicensed band, co-channel interference caused by frequency collisions among coexisting networks have become one of the major performance limiting challenges. In recent years the coexistence issue has gained increasing attention. However, many collision avoidance schemes are not applicable to multiple frequency hopped (FH) networks, mainly due to that the frequency channels of FH signals are constantly changing and the hop sequence of one network is unknown to another. In this project, we develop a dual channel transmission technique for co-channel interference mitigation and robust coexistence of multiple wireless networks. This report describes					
15. SUBJECT TERMS Frequency hopping, coexistence, co-channel interference, frequency diversity					
16. SECURITY CLASSIFICATION OF:		17. LIMITATION OF ABSTRACT SAR	15. NUMBER OF PAGES	19a. NAME OF RESPONSIBLE PERSON Xiangqian Liu	
a. REPORT U	b. ABSTRACT U			c. THIS PAGE U	19b. TELEPHONE NUMBER 502-852-1559

Report Title

Dual Channel Transmission for Coexistence of Wireless Networks

ABSTRACT

With the upcoming pervasive deployment of wireless networks and devices on the unlicensed band, co-channel interference caused by frequency collisions among coexisting networks have become one of the major performance limiting challenges. In recent years the coexistence issue has gained increasing attention. However, many collision avoidance schemes are not applicable to multiple frequency hopped (FH) networks, mainly due to that the frequency channels of FH signals are constantly changing and the hop sequence of one network is unknown to another. In this project, we develop a dual channel transmission technique for co-channel interference mitigation and robust coexistence of multiple wireless networks. This report describes the system modeling, design, theoretic analysis, simulation, and testbed implementation involved in the aforementioned framework.

List of papers submitted or published that acknowledge ARO support during this reporting period. List the papers, including journal references, in the following categories:

(a) Papers published in peer-reviewed journals (N/A for none)

1. J. Li, X. Liu, and A. Swami, "Collision analysis for coexistence of multiple Bluetooth piconets and WLAN with dual channel transmission," IEEE Trans. Communications, accepted, Jun. 2007.
2. J. Li, X. Liu, and X. Ma, "First-order perturbation analysis of singular vectors in singular value decomposition," IEEE Trans. Signal Processing, to appear, 2008.

Number of Papers published in peer-reviewed journals: 2.00

(b) Papers published in non-peer-reviewed journals or in conference proceedings (N/A for none)

Number of Papers published in non peer-reviewed journals: 0.00

(c) Presentations

Number of Presentations: 0.00

Non Peer-Reviewed Conference Proceeding publications (other than abstracts):

Number of Non Peer-Reviewed Conference Proceeding publications (other than abstracts): 0

Peer-Reviewed Conference Proceeding publications (other than abstracts):

1. J. Li and X. Liu, "A frequency diversity technique for interference mitigation in coexisting Bluetooth and WLAN," Proc. International Conference on Communications (ICC), pp. 5490--5495, Glasgow, Scotland, Jun. 24-28, 2007.
2. J. Li and X. Liu, "Evaluation of co-channel and adjacent channel interference for multiple Bluetooth piconets with dual channel transmission," Proc. IEEE Wireless Communications and Networking Conference (WCNC), pp. 2357--2362, Hong Kong, Mar. 11-15, 2007.
3. J. Li, X. Liu, and X. Ma, "Dual channel transmission for coexistence of Bluetooth piconets with multi-slot packets," Proc. International Symposium on Wireless Pervasive Computing (ISWPC), pp. 389--394, San Juan, Puerto Rico, Feb. 5-7, 2007.
4. J. Li and X. Liu, "A collision resolution technique for robust coexistence of multiple Bluetooth piconets," Proc. the 64th IEEE Vehicular Technology Conference (VTC), Sep. 25-28, 2006.

Number of Peer-Reviewed Conference Proceeding publications (other than abstracts): 4

(d) Manuscripts

1. J. Li and X. Liu, "A single-antenna multi-carrier diversity technique for frequency selective fading channels," International Journal of Communication Systems, submitted, Jul. 2007.

Number of Manuscripts: 1.00

Number of Inventions:

Graduate Students

<u>NAME</u>	<u>PERCENT SUPPORTED</u>
Jingli Li	1.00
FTE Equivalent:	1.00
Total Number:	1

Names of Post Doctorates

<u>NAME</u>	<u>PERCENT SUPPORTED</u>
FTE Equivalent:	
Total Number:	

Names of Faculty Supported

<u>NAME</u>	<u>PERCENT SUPPORTED</u>	National Academy Member
Xiangqian Liu	0.10	No
FTE Equivalent:	0.10	
Total Number:	1	

Names of Under Graduate students supported

<u>NAME</u>	<u>PERCENT SUPPORTED</u>
FTE Equivalent:	
Total Number:	

Student Metrics

This section only applies to graduating undergraduates supported by this agreement in this reporting period

- The number of undergraduates funded by this agreement who graduated during this period: 0.00
 - The number of undergraduates funded by this agreement who graduated during this period with a degree in science, mathematics, engineering, or technology fields:..... 0.00
 - The number of undergraduates funded by your agreement who graduated during this period and will continue to pursue a graduate or Ph.D. degree in science, mathematics, engineering, or technology fields:..... 0.00
 - Number of graduating undergraduates who achieved a 3.5 GPA to 4.0 (4.0 max scale):..... 0.00
 - Number of graduating undergraduates funded by a DoD funded Center of Excellence grant for Education, Research and Engineering:..... 0.00
 - The number of undergraduates funded by your agreement who graduated during this period and intend to work for the Department of Defense 0.00
 - The number of undergraduates funded by your agreement who graduated during this period and will receive scholarships or fellowships for further studies in science, mathematics, engineering or technology fields: 0.00
-

Names of Personnel receiving masters degrees

NAME

Total Number:

Names of personnel receiving PHDs

NAME

Jingli Li

Total Number:

1

Names of other research staff

NAME

PERCENT SUPPORTED

FTE Equivalent:

Total Number:

Sub Contractors (DD882)

Inventions (DD882)

TECHNICAL REPORT

W911NF-06-1-0415

Dual Channel Transmission for Coexistence of Wireless Networks

September 1, 2006 – August 31, 2007

Xiangqian Liu, PI

Department of Electrical and Computer Engineering

University of Louisville, Louisville, KY 40292

Tel: 502-852-1559, Fax: 502-852-6807

Email: x.liu@louisville.edu

Contents

A Project Abstract	1
B Problem Statement	1
C Main Contributions	2
D Prior Work	3
D.1 Collaborative Mechanisms	3
D.1.1 MAC Enhanced Temporal Algorithm (META)	3
D.1.2 Alternating Wireless Medium Access (AWMA)	4
D.1.3 Deterministic Frequency Nulling Scheme (DFNS)	5
D.1.4 Coordinated Co-located Access Point (CCAP)	5
D.2 Non-collaborative Mechanisms	6
D.2.1 Adaptive Frequency Hopping (AFH)	6
D.2.2 Bluetooth Interference Aware Scheduling (BIAS)	8
D.2.3 Overlap Avoidance (OLA)	8
D.2.4 Power Control Scheme Based on SIR	10
D.2.5 A Hybrid Scheme	10
E Dual Channel Transmission	11
E.1 Analysis for Coexistence of Multiple Bluetooth Piconets	12
E.1.1 Analysis for Piconets with the Same Packet Type	13
E.1.2 Analysis for Piconets with Mixed Packet Type	16
E.1.3 Simulations and Discussion	18
E.2 Coexistence of Multiple Bluetooth Piconets and a WLAN	20
E.2.1 Performance Analysis	20
E.2.2 Simulations and Discussion	21
E.3 Performance in Realistic Scenario	21
E.3.1 Performance Analysis	22
E.3.2 Simulations and Discussion	25
F A Single-Antenna Multi-Carrier Diversity Method	25
F.1 System Model	26
F.1.1 The Channel Model	26
F.1.2 The Multi-Carrier Diversity System	27
F.1.3 Complex-Field Coding for Channel Diversity	28
F.2 Performance Analysis	30
F.2.1 System Model for Uncoded/Coded OFDM	30
F.2.2 Comparison of MCS/MCC and OFDM for Uncoded Case	31
F.2.3 Comparison of MCS/MCC and OFDM for Coded Case	33
F.3 Simulations and Discussion	34

F.4 Application to the DCT Design	35
G Conclusions	36
H Bibliography	37

List of Figures

1	Time segmentation of the WLAN and Bluetooth intervals in AWMA.	4
2	The adaptive hop selection mechanism.	7
3	An example for D-OLA transmission.	9
4	The diagram for dual hop sequence generation.	11
5	Multi-slot packets.	12
6	PER for versus E_b/N_0 : (a) one-slot packet; (b) five-slot packet.	18
7	Performance for piconet with one-slot packet: (a) PER; (b) throughput.	19
8	(a) Average packet transmission time. (b) PER for frequency diversity methods on different number of channels.	19
9	Performance for mixed packet type case: (a) PER; (b) throughput.	19
10	Performance when coexist with a WLAN: (a) PER; (b) throughput.	21
11	An example geometrical arrangement in the local area.	22
12	Performance in realistic case: (a) PER; (b) throughput.	26
13	The system block diagram for MCS method with two channels.	29
14	Local power ratio for: (a) the selection diversity system; (b) the combining diversity system.	32
15	Performance comparison: (a) the uncoded case; (b) the case with CFC.	34
16	PER in fading channels when number of piconets is (a) 2; (b) 10.	36

A Project Abstract

With the upcoming pervasive deployment of wireless networks and devices on the unlicensed band, co-channel interference caused by frequency collisions among coexisting networks have become one of the major performance limiting challenges. In recent years the coexistence issue has gained increasing attention. However, many collision avoidance schemes are not applicable to multiple frequency hopped (FH) networks, mainly due to that the frequency channels of FH signals are constantly changing and the hop sequence of one network is unknown to another. In this project, we develop a dual channel transmission technique for co-channel interference mitigation and robust coexistence of multiple wireless networks. This report describes the system modeling, design, theoretic analysis, simulation, and testbed implementation involved in the aforementioned framework.

B Problem Statement

Wireless networking is revolutionizing the way people work and play. By removing physical constraints commonly associated with high-speed networking, individuals are able to use networks in ways never possible in the past. Frequency hopping spread spectrum (FHSS) is widely used for radio transmission in such networks, due to its low probability of detection/interception [1]. For example, FHSS is adopted in the single channel ground-airborne radio system (SINCGARS), which is the current standard army combat net radio. Recently FHSS has also been adopted in commercial applications such as HomeRF [2] and Bluetooth [3].

In FHSS systems, the available channel bandwidth is divided into multiple frequency channels. The data signal is modulated with a carrier frequency that hops from one channel to another at a regular interval as a function of time. Frequency hopping is robust to frequency-selective channel fading, and it does not require stringent power control to alleviate the near-far problem as needed for direct sequence spread spectrum (DSSS) systems. A hop sequence, also called hop code or hop pattern, determines the frequencies a user will transmit and in which order. To properly receive a frequency hopped (FH) signal, the receiver must know the transmitter's hop sequence and hop timing.

A Bluetooth piconet is taken as the example of a typical FH network. The Bluetooth transceiver operates in the unlicensed 2.4 GHz industrial, scientific and medical (ISM) band, where signals can hop among 79 frequency channels between 2.4 GHz and 2.480 GHz with 1 MHz channel spacing. The nominal hop rate is 1600 times per second. A Bluetooth piconet is formed when one master device and up to seven slave devices are connected via Bluetooth technology. Each piconet has a unique hop sequence that is determined by the address and clock of the master device. A time division duplex (TDD) scheme is used for the master and slave devices to transmit alternatively.

Because of their increasing deployment, multiple (homogeneous and/or heterogeneous) wireless networks with overlapping frequency bands are likely to coexist in a physical environment, especially in tactical operations, emergency situations, or dense-populated areas. Consequently co-channel interference due to frequency collisions can become a major performance limiting factor [4–6]. When collisions occur, network throughput decreases and delay can become excessive due to retransmissions. Theoretical analysis has shown that the packet error rate (PER) of one Bluetooth piconet due to collisions can be up to 10% if seven piconets coexist [7], and a Bluetooth receiver may experience up to 27% packet loss for data traffic and 25% packet loss for voice applications in the presence of interference from an IEEE 802.11b based WLAN [8].

Recently the coexistence issue has gained increasing attention [9–15]. However, to date most coexistence schemes are designed for simultaneous functionality of a Bluetooth piconet and an 802.11b WLAN. The latter is a direct sequence spread spectrum network that occupies a fixed frequency band of 22 MHz. The

collision avoidance techniques can be classified as collaborative and non-collaborative ones. For the collaborative case, attractive data transmission rates and throughput can be achieved by using a communication link between the Bluetooth and WLAN when they are embedded on the same device [16] or by coordinating the hop frequencies of the co-located Bluetooth devices [9]. However, the center control mechanism needed for collaborative schemes confines their applications to certain situations. Non-collaborative methods [10–15, 17, 18] do not require direct communication between the two networks, and they usually rely on monitoring the channel to detect interference and estimate traffic. These methods are not applicable to the coexistence of multiple FH networks, because the frequency channels are constantly changing and the hop sequence of one network is unknown to another.

Instead of avoiding the collision by scheduling, many efforts have been made on interference suppression and mitigation on physical layer. The problem is challenging because when multiple FH wireless networks coexist in noncooperative scenarios, not only the hop sequences, hop timing/rate and other parameters such as hop bandwidth and bin-width are unknown to each other. Additionally, there may be model order variations even if the number of active emitters remains the same. If the receiver’s bandwidth is not matched to the hop bandwidth of the emitters, the FH signals will hop in and out of the observation frequency band of the receiver.

Another important feature of modern communications is high data rate transmission. A major challenge in high rate data transmission over radio channels is to overcome the signal corruption caused by multipath propagation. If the delay spread of the multipath dispersion exceeds the symbol period, symbols will be affected by intersymbol interference (ISI) and the number of affected symbols grows linearly with the data rate. Since the channel frequency response exhibits significant amplitude fluctuation over frequency, wireless channel with this characteristic is termed frequency-selective channel. Severe attenuation makes it impossible for the receiver to determine the transmitted signal unless some less-attenuated replica of the transmitted signal is provided to the receiver. This resource is called diversity [19]. It is observed that if two or more radio channels are sufficiently separated in frequency, the fading on the various channels is more or less independent [20].

Many techniques use multiple antennas to introduce signal diversity in order to compensate for unacceptable signal fades experienced on frequency-selective wireless communication channels. For example, a transmit diversity scheme is proposed in [21]. This scheme is similar to Alamouti’s space-time codes [22] with two transmit antennas and one receive antenna, but it can handle channels with ISI. [23] provides a frequency domain equalizer with diversity technique. It performs maximum ratio combining of the spectra of two diversity branches and eliminates ISI using zero-forcing equalization. However, multiple antennas typically imply increased size and cost. The use of multiple antennas may not be possible in many applications where devices have strict size constraint, since a minimum physical separation is needed between different antennas to achieve spatial diversity. We propose a single-antenna multi-carrier diversity method, which can be applied to the DCT technique to effectively combat fading and to improve the performance for high rate data transmission.

C Main Contributions

The main contributions of our work can be summarized as follows:

1. A dual channel transmission method is proposed for co-channel interference mitigation and robust coexistence of multiple FH networks. Performance analysis for the coexistence of multiple Bluetooth piconets and/or WLAN is provided based on the following metrics: packet error rate, throughput, and

transmission time. An analysis considering realistic wireless characteristics such as the geometry of the environment, the position of the receiver, the propagation characteristics and the adjacent channel interference is given. Pertinent implementation issues are discussed. Comparisons to single channel transmission and adaptive frequency hopping are performed.

2. A single-antenna multi-carrier diversity combining technique is developed for FH networks to enhance high data rate transmission. Performance evaluation and theoretical analysis are presented to prove the effectiveness of this technique. It is applied to the dual channel transmission method to improve the performance for data transmission in frequency-selective channels when multiple FH networks coexist.

D Prior Work

D.1 Collaborative Mechanisms

Based on the direct communication coexisting network and a central control scheme, collaborative mechanisms achieve attractive data transmission rates and throughput. But the central control mechanism needed for collaborative schemes confines their applications to certain situations. Four collaborative techniques: the MAC enhanced temporal algorithm (META) [24], the alternating wireless medium access (AWMA) [16], the deterministic frequency nulling scheme (DFNS) [25] and the coordinated co-located access point (CCAP) scheme [9] are described in the following.

D.1.1 MAC Enhanced Temporal Algorithm (META)

META [24] is an intelligent scheduling algorithm with queuing aimed to facilitate collaborative coexistence between Bluetooth and WLAN, as well as among Bluetooth piconets/scatternets. The META [24] assumes that the Bluetooth and WLAN are collocated in the same device and they can communicate with each other. A centralized MAC layer controller monitors the Bluetooth and WLAN traffic and predicts collisions. The MAC layer coordination allows precise timing of packet traffic. Each attempt to transmit by either the Bluetooth or the WLAN is submitted to META for approval. If it foresees that a collision will happen, it schedules proper transmission activities for both Bluetooth and WLAN to execute. META can deny a transmit request that would result in collision.

Specifically, the META control entity receives a per-transmission transmit request and issues a per-transmission transmit confirm to each stack to indicate whether the transmission can proceed. The transmit confirm signal carries a status value that is either allowed or denied. The transmit request and confirm signals are exchanged for every packet transmission attempt. By using META, Bluetooth and WLAN transmit their packets sequentially according to the schedule, collisions are avoided. The schedule that which one transmits after another is made based on the packet types. For example, WLAN acknowledgment packets have the highest priority and the Bluetooth SCO traffic has higher priority than WLAN data packets. That is, if a WLAN acknowledgment packet is to collide with a Bluetooth packet, Bluetooth should delay its transmission. If a Bluetooth SCO packet is about to collide with a WLAN data packet, WLAN should delay its transmission.

Simulation results in [24] show that during Bluetooth ACL operation, META optimizes WLAN throughput, and during Bluetooth SCO operation, it attempts to improve SCO performance, even if it reduces WLAN throughput. META meets required Bluetooth and WLAN timing constraints, eg., the acknowledg-

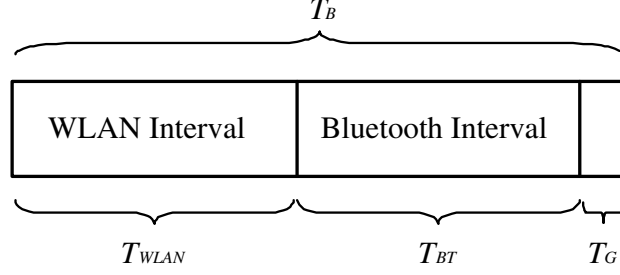


Figure 1: Time segmentation of the WLAN and Bluetooth intervals in AWMA.

ment (ACK). No modification in the physical layer is required with META. It supports both ACL and SCO links in Bluetooth. But it introduces some latency due to the delay of transmission.

D.1.2 Alternating Wireless Medium Access (AWMA)

AWMA [16] is a MAC layer mechanism that is based on TDMA. It assumes that the Bluetooth radio and the WLAN radio are collocated in the same physical unit. In order to avoid overlap in time between their transmissions, the Bluetooth and WLAN devices transmit alternately according to their assigned time intervals.

A WLAN sends out beacons periodically. Let us denote the beacon period as T_B . T_B is split into three subintervals in AWMA: the WLAN subinterval T_{WLAN} , the Bluetooth subinterval T_{BT} and the guard interval T_G . The guard interval is optional, it may be used to guarantee that all Bluetooth traffic has completed before the next beacon is sent. Fig. 1 illustrates the time segmentation of the WLAN and Bluetooth intervals. T_{WLAN} , T_{BT} and T_G are specified by the medium sharing element (MSE) in the beacon. The time allocation for Bluetooth and WLAN intervals obeys the following rules:

1. $T_{WLAN} + T_{BT} \leq T_B$.
2. If $T_{WLAN} > T_B$, $T_{BT} = 0$.
3. If $T_{WLAN} + T_{BT} > T_B$, $T_{BT} = T_B - T_{WLAN}$.
4. If $T_G \neq 0$ and $T_B - T_{WLAN} - T_{BT} < T_G$, $T_{BT} = T_B - T_{WLAN} - T_G$.
5. If $T_{WLAN} < T_B$ and $T_{WLAN} + T_G \geq T_B$, $T_{BT} = 0$.

Because the Bluetooth master and the WLAN node are collocated in the same physical unit, the WLAN node can control the timing of the Bluetooth and WLAN. AWMA requires the WLAN node to send a synchronization signal to the Bluetooth master. This signal contains the specification for the Bluetooth interval and the WLAN interval. Management of the AWMA coexistence mechanism is handled over the WLAN by utilizing the MSE in the beacon.

The performance analysis of WPAN and WLAN utilizing AWMA is also provided in [16]. The results are highlighted here. The Bluetooth throughput with AWMA enabled is the throughput of the Bluetooth with no WLAN present multiplied by T_{BT}/T_B . Similarly, the WLAN throughput with AWMA enabled is the throughput of the WLAN with no WPAN present multiplied by T_{WLAN}/T_B . The AWMA coexistence mechanism also increases the latency of each packet sent over the WPAN and WLAN networks. The

extra latency introduced by AWMA over the Bluetooth transmission is $T_{WLAN}^2/2$, while the extra latency introduced by AWMA over the WLAN transmission is $T_{BT}^2/2$.

By scheduling the WLAN and the Bluetooth radio transmissions, the AWMA coexistence mechanism prevents CCI between WLAN and Bluetooth. It is recommended to use AWMA when the density of devices with collocated Bluetooth and WLAN is high, or when the Bluetooth and/or WLAN bandwidth allocation needs to be deterministically controlled irrespective of its traffic load. Note that the AWMA mechanism can not be applied to the case when SCO links is utilized in Bluetooth.

D.1.3 Deterministic Frequency Nulling Scheme (DFNS)

The DFNS [25] is a collaborative method for collocated Bluetooth and WLAN devices. It aims to mitigate the effect of Bluetooth on WLAN. It is primarily a physical layer solution. By employing a Bluetooth receiver as part of the WLAN receiver, the WLAN receiver can obtain the hop frequencies, hop timing and hop pattern of the Bluetooth transmitter. Because WLAN occupies approximately 22 MHz bandwidth and Bluetooth occupies approximately 1 MHz bandwidth at each hop, the Bluetooth signal can be assumed as a narrowband interferer for WLAN. Then WLAN can put a null in its receiver at the frequency of the Bluetooth signal in order to suppress the interference from Bluetooth.

The implementation of DFNS is described as following. Between the chip matched filter and the PN correlator in the WLAN device, there is an adjustable transversal filter. The optimal coefficients of this filter are estimated and then used to update the filter. By assuming that the interferer is a pure tone and that the PN sequence is sufficiently long, the PN signal samples at the different taps are considered to be uncorrelated and the solutions for the optimal tap weights are simply related to the signal power, the interferer power, the noise power, and the frequency of the interferer. Because the interfering frequency is assumed known a priori and the SNR is often quite high for WLAN systems, only an estimation of the carrier-to-interference (CIR) ratio is necessary to determine the optimal tap coefficients.

The bit error rate (BER) performance analysis in [25] for a 1 Mb/s WLAN system in an AWGN channel with Bluetooth interference shows that the performance of WLAN is greatly improved by using DFNS. As the Bluetooth frequency is known, the offset between the WLAN and the interferer can be calculated. As shown in the experiments in [25], without using DFNS, the BER is 5% for a 5 MHz offset at approximately -11 dB CIR. With DFNS, even for the worst case of a 1 MHz offset, a CIR of -20 dB can achieve a BER less than 0.1%.

Unlike META and AWMA, DFNS causes no delay for the transmission. Because the frequencies of Bluetooth may not always fall into the WLAN band, in META and AWMA, the bandwidth is not fully utilized as in DFNS. By using DFNS, the total data throughput for WLAN increases because there is no packet loss or retransmission due to collision.

D.1.4 Coordinated Co-located Access Point (CCAP)

The CCAP [9] scheme reduces CCI in co-located Bluetooth devices by coordinating their hopping frequencies in a scatternet scenario. A group of piconets in which connections exist between different piconets is called a scatternet [3]. In a scatternet, slaves can participate in different piconets on a time-division multiplex basis. Slave E is an example for this case. In addition, a master in one piconet can be a slave in other piconets. For example, device B is the master of piconet B and also a slave in piconet A. In the Bluetooth specification [3], piconets shall not be frequency synchronized and each piconet has its own hopping sequence. As shown in [9], by breaking this rule and using CCAP, there can be a significant gain in capacity

and throughput.

It is defined in [9] that the co-located devices forming a Bluetooth AP are essentially the masters of the piconets which they form. The CCAP technique operates by coordinating hop frequency selection between co-located master nodes. First, the hop timings of the master nodes are synchronized, then the same hopping sequence with different frequency offset is applied to each master node. Therefore no two devices use the same frequency at the same time and CCI is eliminated between Bluetooth piconets. Because the frequency hopping sequence for Bluetooth is uniquely determined by the Bluetooth device address and the clock counter, the coordination of the hop frequency selection can be done in two different methods. The first method is to let every piconet use the same device address and clock counter to generate the same hopping sequence and add multiples of a fixed frequency offset to each hopping sequence. The second method is to add offsets to the clock counter, so that there will be frequency offset in the output of each hopping sequence. Note that the offsets for the clock counter should be predetermined. A universally available device address of 0x000000 is suggested in [9].

In Bluetooth, a control protocol for the baseband and physical layers is carried over logical links in addition to user data. This is the link manager protocol (LMP) [3]. Devices that are active in a piconet have a default asynchronous connection-oriented logical transport that is used to transport the LMP protocol signalling. It is pointed out in [9] that some interference can occur when the LMP signaling takes place. This problem can be alleviated by using clock offsets that are not closely spaced. Interference is also possible when the nodes of a CCAP system are in an inquiry or paging state. This interference can be reduced if the least loaded node of the AP is required to enter the inquiry or paging scan state frequently, in order to respond to potential clients in the shortest possible time [9]. By using CCAP in the connection state, no CCI occurs when all master nodes use packets of the same length. The capacity and throughput of the Bluetooth networks is greatly increased when compared to conventional Bluetooth. In addition, because of the known address used, the handover time can be decreased considerably by using CCAP.

D.2 Non-collaborative Mechanisms

Non-collaborative mechanisms do not require direct communication between two coexisting networks so that they provide more flexibility for implementation, but most of them may rely on monitoring the channel to detect interference and estimate traffic. Since a variety of mechanisms are embraced in this category, in the following, we only describe several typical mechanisms in detail.

D.2.1 Adaptive Frequency Hopping (AFH)

We begin with a description of AFH [3, 12], one of the most widely adopted coexistence mechanisms. The idea of AFH is that Bluetooth devices can maintain a performance measurement for each channel visited, and periodically classify “good” and “bad” frequency channels, then modify their hop patterns to avoid frequency bands occupied by a WLAN. Because a WLAN usually occupies a fixed frequency band for a relatively long time, it is possible to monitor/detect frequencies occupied in this band by performance measurement.

Interference estimation can be performed by measuring the signal-to-interference ratio (SIR), BER, packet loss, or frame error rate in a Bluetooth receiver. Here PER measurement is adopted. If the PER on certain carrier frequency is greater than the packet loss threshold 0.5, this frequency is considered to be a bad frequency, otherwise, it is considered to be a good one. Because the master in a Bluetooth piconet is in charge of all packet transmissions, the channel information collected by the slave must be made available

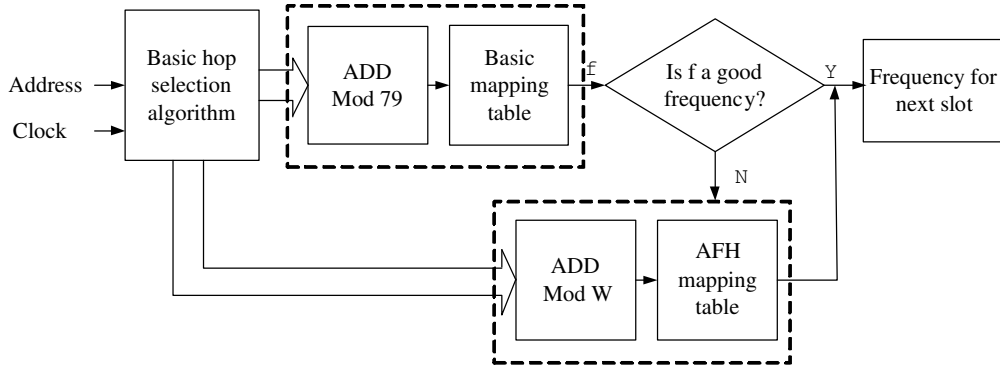


Figure 2: The adaptive hop selection mechanism.

to the master. One way to achieve this is that the master and the slave exchange channel information via management messages periodically. Another way is that the master makes use of the acknowledgement information in each slave's response packets to determine the channel information. The second way can speed up the estimation time. It is important to remark that there is a tradeoff between the classification update interval and the performance improvement. A higher update rate can capture rapid environment changes thus guarantee channel information accuracy. But it incurs a higher communication overhead if the information is distributed via management messages.

Frequency hopping in traditional Bluetooth is executed as follows. 79 carrier frequencies are sorted into a list of even and odd frequencies in the 2.402-2.480 GHz range, with all the even frequencies followed by all the odd frequencies. A segment consisting of the first 32 frequencies in the sorted list is chosen. After all 32 frequencies in that segment are visited once in a random order, a new segment is set including 16 frequencies of the previous segment and 16 new frequencies in the sorted list. In AFH, bad frequencies are eliminated in the sequence. Given a segment of 32 good and bad frequencies, each good frequency is visited exactly once. While each bad frequency in the segment is replaced with a good frequency selected from outside the original segment of 32. Due to the FCC regulation, at least 15 different frequencies should be kept in the hop sequence. If there are less than 15 good frequencies left, some of the bad frequencies will be used.

AFH requires modification of the original Bluetooth specification, this has already been turned into reality in the updated version of Bluetooth specification [3]. The adaptive hop selection mechanism in [3] is shown in Fig. 2. When AFH is enabled in a Bluetooth device, the basic hop selection procedure for conventional Bluetooth is initially used to determine a hop frequency. Parameters generated by the basic hop selection algorithm from the clock and the address of the master are sent to the basic hop selection kernel, where a frequency is selected from the 79 frequencies in the basic mapping table. If this frequency is a good frequency, no adjustment is made, and it is used as the frequency for the next packet. If it is a bad frequency according to the channel classification information, the frequency is replaced with a good frequency by executing the re-mapping function. A good frequency is selected from the AFH mapping table which consists U good frequencies, and this new frequency is used as the frequency for the next packet. Since only bad frequencies are replaced by new frequencies, good frequencies remain unchanged in the hop sequence, non-AFH slaves remain synchronized while other slaves in the piconet are using the adapted hopping sequence [3].

In order to keep all devices in the piconet updated with the new hopping pattern, advertisement of the new hopping sequence is typically done by using LMP messages exchanged between the master and slaves

in the piconet. How often a new hopping pattern should be advertised could be dynamically adjusted so that it tracks changes in the channel.

Performance evaluation results of AFH are provided in [12] for FTP and voice applications. Maximizing the throughput is the goal for FTP application and minimizing the delay is the goal for voice application. AFH improves the throughput by 25 percent for FTP application. The improvement is more obvious than that for voice application. When Bluetooth and WLAN coexist, the PER for WLAN drops if AFH is adopted. AFH allows additional scheduling techniques to be used simultaneously if there is a need to control the transmission of packets on the medium. AFH has been demonstrated effective in dealing with static interference comes from WLAN, but it is not applicable for multiple co-located Bluetooth piconets, because in Bluetooth, frequency channels are constantly changing, the hop pattern of one piconet is not known to another one, and multiple piconets are not necessarily synchronized in a typical non-collaborative scenario. Besides, the performance of AFH is also dependent on the update rate of the frequency classification to track the channel dynamics [12].

D.2.2 Bluetooth Interference Aware Scheduling (BIAS)

By taking advantage of the fact that devices in the same piconet are not subject to the same levels of interference on all channels of the band, the BIAS [26] algorithm dynamically distributes channels to devices in order to maximize their throughput while maintaining fairness of access among users.

Interference estimation is used to identify whether a frequency is good or bad based on SIR or PER measurement. The estimation and classification is done continuously. The master collects frequency classification information and schedules the transmission about sending packet to which slave and using which frequency. Before each transmission, the master chooses a slave device if no retransmission is required at that moment. Then the master verifies whether the two frequencies that will be used by itself and the slave device are good frequencies. The new transmission will begin only if both frequencies are good. Otherwise, the master postpones the transmission of the packet until a good pair of frequencies becomes available. When the master schedules transmission, retransmission has the highest priority and is transmitted first, then data packets and finally the acknowledgment packets are transmitted. In all cases, the frequency pair must consist with good frequencies. In Bluetooth, a slave device must respond to the master device even if it does not have any data to send (in this case, a NULL packet will be sent). Therefore a slave transmission always follows a master transmission. When using BIAS, the master avoids receiving data on a “bad” frequency, by avoiding a transmission on a frequency preceding a “bad” one in the hopping pattern.

BIAS needs to be implemented in the master device only. It adopts a backoff strategy for Bluetooth to avoid collision with WLAN. BIAS is a neighbor-friendly strategy for WLAN because it avoids transmission on WLAN band. BIAS may outperform AFH for delay jitter and packet loss constrained applications such as voice and video [12]. Performance results obtained in [26] show that BIAS eliminates packet loss of Bluetooth even in the worst interference case when more than 3/4 of the spectrum are occupied by other networks. The increased delay compared to the case that no interference is present varies between 1 to 5 ms on average. Furthermore, BIAS is adaptable to rapid changes of the channel. But it is not very effective to mitigate interference comes from other Bluetooth piconets.

D.2.3 Overlap Avoidance (OLA)

The OLA scheme [13] assumes that Bluetooth and WLAN devices can acquire the interference information from each other by channel sensing, PER calculation and received signal power monitoring in a non-collaborative scenario. It can also be used in collaborative scenario by assuming that the traffic information

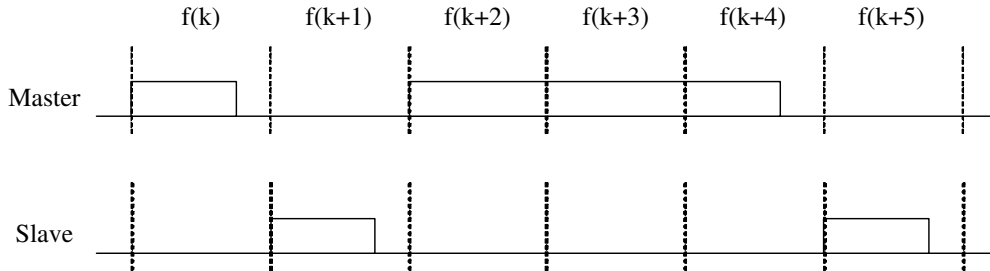


Figure 3: An example for D-OLA transmission.

is exchanged between WLAN and Bluetooth. The basic idea of this scheme is traffic scheduling at the MAC layer. It consists of voice-OLA (V-OLA) to deal with Bluetooth voice traffic and data-OLA (D-OLA) to deal with Bluetooth data traffic. The two algorithms are jointly applied when both voice and data are transmitted in Bluetooth devices.

For Bluetooth voice traffic, SCO link is adopted. Packets are transmitted in a predetermined pattern. The channel idle time also obeys a deterministic pattern. By taking advantage of the fixed pattern, WLAN packets are scheduled to be transmitted with an adjusted length and during the Bluetooth channel idle time. This is how V-OLA works. V-OLA is still applicable when there are both SCO and ACL links by assuming that the CCI caused by ACL traffic is negligible compared to the CCI caused by SCO traffic. When the channel is occupied, the WLAN can choose to transmit a shortened packet (named the shortened transmission (ST) mode) or delay the transmission (named the postponed transmission (PT) mode). When dealing with the detection of the ending time of SCO, it is pointed out in [13] that the WLAN considers the Bluetooth SCO transmission ends if it does not detect any interference for a certain time period. Note that the timing of the Bluetooth packet transmission may drift so that imperfect information may be obtained.

For Bluetooth data traffic, ACL link is adopted. D-OLA is employed by assuming that the Bluetooth master has the information about the frequency bands occupied by WLAN. If the next Bluetooth carrier frequency falls into the WLAN band, the Bluetooth master will schedule to transmit a long packet using the current carrier frequency. Therefore the next carrier frequency is skipped and CCI is eliminated. Fig. 3 gives an example. Suppose that $f(k+3)$ falls into the WLAN band, the master knows this and chooses to transmit a three-slot packet instead of a single-slot packet, so that transmission on frequency $f(k+3)$ is avoided. This method works on the condition that enough data are buffered for transmission. If there is not enough data, the transmission that causes CCI can be postponed. By taking advantage of the variety of packet lengths and scheduling a packet with proper duration, collision is avoided. According to the FCC regulation, the average occupation time of any frequency should not greater than a threshold. Sometimes, an intelligent schedule is required to use some of the bad frequencies while maximizing the usage of all the good frequencies.

Performance results in [13] show that OLA greatly improves the system throughput. V-OLA PT causes more delay for WLAN than V-OLA ST does, while D-OLA does not cause much delay for Bluetooth. When operating in the case that interfering devices are collocated in the same physical unit, collaborative methods such as META outperforms OLA. With non-collocated interfering devices, OLA outperforms META. The OLA scheme only requires a minor change on the Bluetooth standard and the 802.11 specification. It not only avoids overlap between Bluetooth and WLAN but also copes with interference comes from microwave ovens, which also operates at 2.4 GHz band.

D.2.4 Power Control Scheme Based on SIR

Provided that Bluetooth devices can dynamically change their transmission power, a power control scheme based on the SIR is proposed in [11]. Since no information about other systems is available in the Bluetooth receiver, it can only measure the interference to obtain the SIR. Based on each measurement, the current power is updated by multiplying itself with a ratio. The ratio is the target SIR divided by the measured SIR. With the target SIR, the signal power level is adjusted to no more than what is needed. The updated power is bounded by the minimum and maximum transmission power range. If there is no change in the interfering signal, the transmitted power can converge to its final value in one step.

Bluetooth transmitter has three levels of radio transmission power: 100 mW (20 dBm), 2.5 mW (4 dBm) and 1 mW (0 dBm). Power control method only works well for the first two cases since the maximum power of 1 mW limits the power changing range. The Bluetooth specification [3] suggests that the transmitted power should be adjusted based on the received signal strength indicator (RSSI) measurements at the receiver. By assuming that the noise can be neglected, RSSI corresponds to the SIR. LMP messages are used to transmit the measured SIR from the receiver to the transmitter so that it can perform the power updating. It is pointed out in [11] that there is a tradeoff between the value of the update interval and the signalling traffic required. A small value of the update interval makes the system more adaptive but requires more signalling information to be exchanged.

Experimental results are reported in [11]. The maximum power for Bluetooth is set to 100 mW. The WLAN power is set to 25 mW. By using power control, the PER for Bluetooth decreases from 18% to 4% when the distance between Bluetooth and WLAN is 0.5 m. Bluetooth with power control effectively reduces PER for distance greater than 0.5 m. But when the distance is less than 0.5 m, since the transmitted power is bounded by the maximum power, it can not achieve further performance improvement.

The power control scheme does not change the Bluetooth frequency hopping pattern. It requires no change in the Bluetooth specification. It can be easily implemented by using a scheduling rule on current Bluetooth chip set. It is compatible to devices without power control. The power control scheme is effective in the scenario that the interference power is not too large, because the maximum achievable SIR is limited by the maximum transmission power. What's more, increasing the Bluetooth transmission power will inevitable incur more interference to neighboring devices.

D.2.5 A Hybrid Scheme

A hybrid scheme which combines power control, LBT and AFH to achieve low PER and improve system throughput is proposed in [15]. AFH and power control methods are discussed above. LBT is a carrier sense technique. Before each transmission, the transmitter senses the channel in the turn around time of the current slot. If it detects that the channel is occupied, it will postpone its current transmission till another chance. LBT combats dynamic frequency interference by withdrawing packet transmission that may become potential interference. As pointed out in [15], even with ideal carrier sense of Bluetooth, LBT can not totally avoid all packet collisions between Bluetooth and WLAN. LBT can effectively avoid the collision when the Bluetooth packet is to be transmitted during the WLAN transmission duration. If a WLAN begins its transmission in the middle of a Bluetooth transmission and causes collision, LBT can not avoid it. By avoiding hopping into WLAN band, AFH effectively deals with this static interference. Since there are more Bluetooth transmissions outside the WLAN band, if several Bluetooth piconets coexist with a WLAN, AFH may introduce more dynamic frequency interferences to neighboring Bluetooth piconets. Performance results in [15] show that by combining LBT and AFH together, the Bluetooth throughput is increased than using these methods separately, when there are less than 70 Bluetooth piconets coexist with

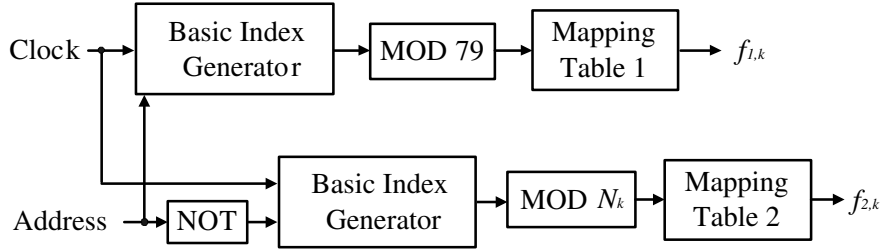


Figure 4: The diagram for dual hop sequence generation.

a WLAN.

By using power control and LBT, unnecessary power usage is avoided. LBT is used to deal with dynamic interference. AFH is used to deal with static interference. The hybrid method is implemented by adding a few extension to the MAC layer and it is compatible with the current Bluetooth specification.

To summarize this section, we note that most non-collaborative methods are applied in Bluetooth to avoid collision with WLAN, because Bluetooth is more vulnerable to CCI if Bluetooth and WLAN coexist. AFH [12] and interference source oriented AFH (ISOAFH) [18] are effective in dealing with WLAN interference, but not applicable for multiple co-located Bluetooth piconets. The performance of AFH is also dependent on the update rate of the frequency classification to track the channel dynamics [12]. Approaches based on scheduling such as BIAS [12, 26], OLA [13] and master delay MAC scheduling (MDMS) [18] cause delay in the transmission, hence they may not be bandwidth efficient. Power control methods [10, 11] depend on the accuracy of channel sensing and can not provide much improvement if the Bluetooth device is very close to the interfering device. Carrier sensing based schemes inevitably suffers from the hidden terminal problem [14, 17]. A hybrid method of power control, LBT and AFH proposed in [15] can achieve better performance with added complexity.

E Dual Channel Transmission

In Bluetooth, packets are transmitted on a frequency bin that hops among $M = 79$ channels at the packet rate. All devices associated with the same piconet share the same hop sequences, which are assumed to be random here for simplicity of analysis as in [27]. Time division is used for multiple access in a piconet. When multiple piconets are within each other's transmission range, a collision occurs when two or more packets are transmitted on the same frequency. A frequency diversity technique is proposed, which uses DCT for Bluetooth piconets to combat CCI. In DCT, the same packet is transmitted on two distinct frequency hopped channels simultaneously and the power used in each channel is half of what would be used in SCT. A packet is successfully received if at least one channel survives. In order to make DCT robust to the $D = 22$ MHz WLAN bandwidth, the two channels of DCT are separated by $\Delta f > 22$ MHz.

The hop sequences for DCT can be generated as shown in Fig. 4. At the k -th hop, one frequency $f_{1,k}$ is generated according to the conventional Bluetooth specification [3], where an index is obtained based on the master device's address and clock (see [3] for details of the basic index generator), then the index modulo M is used to select a frequency from Mapping Table 1. Mapping Table 1 contains M frequencies with all of the even frequencies in ascending order followed by all of the odd frequencies in ascending order. The other frequency, $f_{2,k}$, is generated as follows. Firstly, the master's address is translated to another address (e.g., by taking its complement as shown in Fig. 4). This address and the clock are used to obtain an index from the basic index generator. Mapping Table 2 is obtained by eliminating $f_{1,k}$ and all frequencies with a

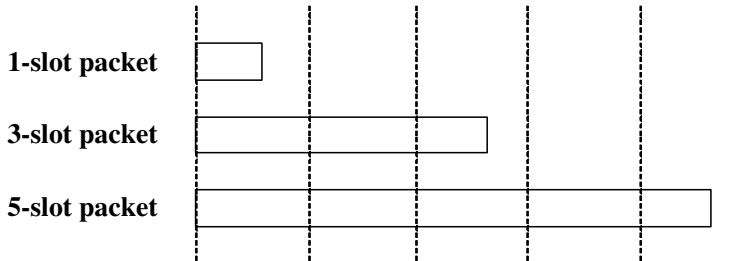


Figure 5: Multi-slot packets.

distance less than D MHz to $f_{1,k}$ from Mapping Table 1. The number of frequencies in Mapping Table 2 is denoted as N_k . The index modulo N_k is subsequently used to select the corresponding frequency from Mapping Table 2 as $f_{2,k}$.

For example, suppose that the frequency $f_{1,k} = 12$ MHz is obtained using the master's address 101 and the clock (for simplicity, a 3 bit device address is used here). The complement of 101 is taken to obtain 010. Since an address in Bluetooth has 28 bits, it is unlikely its complement will result in another address that is already in the system (the probability for two addresses to be identical is $1/2^{28} = 3.7 \times 10^{-9}$). An index is generated from 010 and the clock. Since $f_{1,k} = 12$ MHz, Mapping Table 2 is obtained by eliminating frequencies 1, 2, \dots , 33 MHz from Mapping Table 1. The number of frequencies in Mapping Table 2 is $N_k = 79 - 33 = 46$. Mapping Table 2 has the even frequencies in ascending order followed by the odd frequencies in ascending order as follows: 34, 36, \dots , 78, 35, 37, \dots , 79. Finally $f_{2,k}$ is generated by selecting one frequency from this table according to the index modulo 46.

Here it is assumed that the 1 to 79 MHz frequency bins are equally likely to be overlapped by the 22 MHz WLAN band. In practice, WLAN channels are allocated in a specific way. As listed in table I of [18], the channels of IEEE 802.11b can be centered at 2412 MHz (12 MHz after downconversion), 2417 MHz, \dots , or 2462 MHz respectively, each with a 22 MHz bandwidth. However, PER analysis shows that a uniform distribution assumption is a very close approximation to the practical case with negligible difference.

It is clear that for the same transmitter-receiver link, the received signal power at each channel in DCT is 3 dB less than that of SCT. It will be shown in Section E.1 that at low SNR, when PER is dominated by channel noise, DCT underperforms SCT; when PER is dominated by frequency collisions, DCT outperforms SCT when the number of piconets is less than 20.

E.1 Analysis for Coexistence of Multiple Bluetooth Piconets

In this section, the performance of SCT and DCT when multiple Bluetooth piconets coexist is analyzed. Similar to the analysis for Bluetooth in [7,27], for simplicity, the adjacent channel interference, propagation characteristic, and error correction are not considered. Note that the extension of these results to the case where error correction coding is taken into account can be obtained similar to [4]. Suppose n piconets coexist in sufficiently close vicinity so that a frequency collision in two or more packets for the time duration of at least one bit will destroy all the packets involved. Since there is no coordination between these piconets, each piconet has $n - 1$ potential competitors. Different from [7,27], here the channel noise is also considered. The channel noise is assumed to be AWGN. As shown in Fig. 5, three packet sizes are available for Bluetooth: one-slot, three-slot and five-slot. For a multislot packet, its frequency is determined by the first slot and remains unchanged throughout the packet. For a multislot packet, its frequency is determined by the first slot and remains unchanged throughout the packet. Bluetooth transmissions can occur with a wide variety of

packet combinations. The two main classes of links are known as symmetric and asymmetric. A symmetric link occurs when both the master node and slave node in a piconet transmit packets of the same size. An asymmetric link occurs when the master sends one size packet and receives a different size packet as a response from the slave.

First, the effect of noise on SCT and DCT in AWGN channels is considered. Gaussian frequency shift keying (GFSK) is the modulation format adopted in Bluetooth. The demodulation of GFSK can be approximated as a coherent continuous phase index $h = 0.32$ frequency shift keying (FSK) demodulation. Without CCI, the BER due to noise is given in [28] and shown to be approximately achievable with a zero-IF Bluetooth receiver in [29]

$$P_b(\alpha) = Q\left(\sqrt{\alpha(1 - \text{sinc}(h) \cos(\pi h))}\right), \quad (1)$$

where $Q(x) = \frac{1}{\sqrt{2\pi}} \int_x^\infty e^{-t^2/2} dt$, $\alpha = E_b/N_0$ is the SNR, E_b is the bit energy, and N_0 is the noise power spectral density. The success probability for a k -slot SCT packet with m_k bits is

$$\beta_k(\alpha) = (1 - P_b(\alpha))^{m_k}, \quad (2)$$

where $k = 1, 3, 5$. The success probability of one channel for a k -slot DCT packet with m_k bits is

$$\beta_k(\alpha/2) = (1 - P_b(\alpha/2))^{m_k}, \quad (3)$$

where $\alpha/2$ reflects that the received SNR in each of the two channels in DCT is half of what would be in SCT. Note that in practice, the BER can be inferior to that achieved by the optimal coherent scheme depending on the actual detectors used [30].

E.1.1 Analysis for Piconets with the Same Packet Type

In this section, the case that all piconets use the same type of packets is considered. For one-slot packet, although $625 \mu\text{s}$ is allocated for each packet, the transmission time of a packet is only $366 \mu\text{s}$, and the remaining $259 \mu\text{s}$ idle time is used for transient time-settling. The ratio of the packet to slot duration is $r_1 = 366/625$. For three-slot packets, the ratio is $r_3 = (625 \times 2 + 372)/(625 \times 3)$. For five-slot packets, the ratio is $r_5 = (625 \times 4 + 370)/(625 \times 5)$.

Two extreme cases are considered: one is that all piconets are synchronized, the other is that all piconets are fully unsynchronized, that is, no two piconets are synchronized. If some piconets happen to be synchronized, the PER and throughput will fall within the range of the aforementioned two extreme cases. If piconets are synchronized, a packet of interest may be affected by one packet from each co-located piconet. If piconets are unsynchronized, the packet of interest may be affected by one or two packets from each co-located piconet. The probabilities that there are one or two dangerous packets from a co-located piconet in the unsynchronized case are $2 - 2r_k$ and $2r_k - 1$ respectively [27], where $k = 1, 3, 5$. Assuming a transmission rate of 1 Mbps in each piconet, the average data throughput for each piconet is defined as $(1 - \text{PER})r_k$ Mbps. The throughput includes both original and retransmitted packets.

PER of SCT

When multiple piconets coexist, with SCT a packet is successfully received only when no bit error occurs due to frequency collision or channel noise effect. The PERs for n synchronized and fully unsynchronized piconets with SCT in AWGN channels are

$$P_{sct}^s(k, n) = 1 - s_0^{n-1} \beta_k(\alpha), \quad (4)$$

$$P_{sct}^u(k, n) = 1 - [(2 - 2r_k)s_0 + (2r_k - 1)s_0^2]^{n-1} \beta_k(\alpha), \quad (5)$$

respectively, where $s_0 = (M - 1)/M$ is the probability that one interfering piconet chooses another frequency instead of the one chosen by the piconet of interest. $k = 1, 3, 5$ denotes the packet type. The superscript s in $P_{sct}^s(k, n)$ indicates the synchronized case, and the superscript u in $P_{sct}^u(k, n)$ indicates the fully unsynchronized case.

PER of DCT

With DCT, a packet is successfully received if at least one of the two channels is not destroyed by frequency collisions or channel noise. First, an example of three co-located piconets is used to illustrate the collision analysis for synchronized piconets. Suppose A is the piconet of interest, and B and C are the interfering piconets. Let a_1, a_2 be the two frequencies used in piconet A for a particular packet transmitted. Similarly, let b_1, b_2 , and c_1, c_2 , be the corresponding frequencies in piconets B and C respectively. When three piconets coexist, there are three cases that a packet in piconet A can be successfully received: the first case is that b_1, b_2, c_1 , and c_2 are chosen from frequencies other than a_1 and a_2 ; the second case is that only one of a_1 and a_2 is overlapped by one of the frequencies from b_1, b_2, c_1 , and c_2 ; and the third case is that only one of a_1 and a_2 is overlapped by the same frequency from both B and C : b_1 or b_2 , and c_1 or c_2 . Therefore with DCT, the PER for three synchronized piconets in AWGN is

$$P_{dct}^s(k, 3) = 1 - d_0^2[1 - (1 - \beta_k(\alpha/2))^2] - 4d_1d_0\beta_k(\alpha/2) - 4d_1d_2\beta_k(\alpha/2). \quad (6)$$

In (6), $k = 1, 3, 5$, d_0 is the probability that frequencies of two piconets do not overlap, d_1 is the probability that one frequency of piconet A is overlapped by a frequency of another piconet, and d_2 is the probability that a frequency of piconet C is overlapped with a frequency of piconet A , which is already overlapped by a frequency of piconet B . The functions for d_0, d_1, d_2 are derived in the following.

Note that a_1 and a_2 are the two frequencies selected from the $M = 79$ frequency bins and $|a_1 - a_2| \geq D$ MHz. Specifically, a_1 is uniformly selected from the M frequency bins, a_2 is chosen from Mapping Table 2 which is based on a_1 . Indexes $1, 2, \dots, m, \dots, M$ are used to denote the M frequency bins. For example, 1 is a possible choice for a_2 only if $a_1 = D + 1, D + 2, \dots, M$. Therefore, if a_1 is selected as $1, 2, \dots, M$, then 1 is a possible choice for a_2 for $M - D$ times. Let v_m denote the times that a particular frequency m is a possible choice for a_2 when a_1 is chosen as $1, 2, \dots, M$. It can be verified that

$$v_m = \begin{cases} M - D - m + 1 & \text{for } m = 1, \dots, D, \\ M - 2D + 1 & \text{for } m = D + 1, \dots, M - D, \\ m - D & \text{for } m = M - D + 1, \dots, M. \end{cases} \quad (7)$$

Consequently the probability for $a_2 = i$ is obtained as

$$t_i = \frac{v_i}{\sum_{m=1}^M v_m}, \quad (8)$$

for $i = 1, \dots, M$, which is a nonuniform distribution.

Based on the distribution of the two frequencies for a piconet, it is obtained that

$$d_0 = \sum_{i=1}^M \sum_{j=1}^M \frac{t_j}{M} \left[\frac{M-2}{M} (1 - t_i - t_j) \right], \quad (9)$$

where t_j/M is the average probability for $a_1 = i$ and $a_2 = j$. Also in (9), $(M-2)(1-t_i-t_j)/M$ is the probability for piconet B to choose a frequency pair such that neither b_1 nor b_2 is equal to i and j . Therefore

d_0 can be considered as the probability that four frequencies of piconet A and B are all distinct. Similarly, the probability that either a_1 or a_2 is overlapped by a frequency of piconet B is calculated as

$$d_1 = \frac{1}{2} \sum_{i=1}^M \sum_{j=1}^M \frac{t_j}{M} \left[\frac{2}{M} (1 - t_i - t_j) + \frac{M-2}{M} (t_i + t_j) \right]. \quad (10)$$

Since frequencies of different piconets are generated independently, the probabilities d_0 and d_1 can also be applied for coexistence of piconets A and C . When three piconets coexist, there is a specific case that one frequency of piconet A is overlapped by a frequency of piconet B and also by a frequency of piconet C , which has a probability of $d_1 d_2$, where $d_2 = d_1/2$.

Summarizing the above cases where a packet of piconet A can be successfully received, it can be concluded that the PER of DCT for three synchronized piconets in AWGN is given by (6). (6) is generalized to obtain the PER of DCT for n synchronized piconets in AWGN

$$P_{dct}^s(k, n) = 1 - \sum_{i=0}^{n-1} 2^i \binom{n-1}{i} d_0^{n-1-i} d_1^{\langle i>0} (d_2^{i-1})^{\langle i>1} [1 - (1 - \beta_k(\alpha/2))^2]^{\langle i=0 \rangle} \beta_k(\alpha/2)^{\langle i>0} \quad (11)$$

where $E^{\langle F \rangle}$ is equal to E if F is true, otherwise $E^{\langle F \rangle}$ is equal to 1. In (11), $\binom{n-1}{i}$ is the number of ways of selecting i unordered piconets from $n-1$ piconets, where each selected piconets has one interfering frequency, and 2^i is the number of possible permutations of the interfering frequencies from the i piconets.

Next, the case where the piconets are fully unsynchronized is considered. Suppose i interfering piconets have one dangerous packet, each with probability $2 - 2r_k$, for $i = 0, \dots, n-1$, and the other $n-1-i$ interfering piconets have two dangerous packets, each with a probability of $2r_k - 1$. This is equivalent to that with probability $(2 - 2r_k)^i (2r_k - 1)^{n-1-i}$, there are a total of $1 + i + 2(n-1-i)$ synchronized piconets, which give a PER of $P_{dct}^s(k, 1 + i + 2(n-1-i))$. Therefore the PER of DCT for the fully unsynchronized case is

$$P_{dct}^u(k, n) = 1 - \sum_{i=0}^{n-1} \binom{n-1}{i} (2 - 2r_k)^i (2r_k - 1)^{n-1-i} [1 - P_{dct}^s(k, 1 + i + 2(n-1-i))]. \quad (12)$$

Average Packet Transmission Time

The packet transmission time is defined as the time interval between the start of the packet transmission and the reception of the response ACK. In this section, it is assumed that the packet is continuously retransmitted until an ACK is received (no timeout is considered). Then, the time needed will depend on the number of retries. Based on the derivation in [31], the average packet transmission time for n synchronized and fully unsynchronized piconets with SCT in AWGN channels are obtained as

$$T_{sct}^s(k, n) = 2T_s (1 - P_{sct}^s(k, n))^{-2}, \quad (13)$$

$$T_{sct}^u(k, n) = \sum_{i=0}^{n-1} 2T_s \binom{n-1}{i} (2 - 2r_k)^i (2r_k - 1)^{n-1-i} [s_0^{i+2(n-1-i)} \beta_k(\alpha)]^{-2}. \quad (14)$$

Similarly, for n synchronized and fully unsynchronized piconets with DCT in AWGN channels, the average

packet transmission time is obtained as

$$T_{dct}^s(k, n) = 2T_s(1 - P_{dct}^s(k, n))^{-2}, \quad (15)$$

$$T_{dct}^u(k, n) = \sum_{i=0}^{n-1} 2T_s \binom{n-1}{i} (2-2r_k)^i (2r_k-1)^{n-1-i} (1 - P_{dct}^s[k, 1+i+2(n-1-i)])^{-2}. \quad (16)$$

E.1.2 Analysis for Piconets with Mixed Packet Type

In this section, the collision analysis is generalized to the case of mixed packet type (one-slot, three-slot and five-slot), and the model is similar to [7] except that the AWGN channel is also considered. The system traffic load may vary as idle slots (single-slot with no traffic load) are added into the model.

Based on the result in [7], the PER for SCT is derived firstly. Let $F_{sct}^m(k, n)$ denote the probability of success for k -slot packet in the piconet of interest when n unsynchronized piconets with SCT coexist without noise, where $k = 1, 3, 5$. The superscript m denotes that mixed packet types coexist. Then, the PER for a k -slot packet when n piconets with SCT coexist in AWGN channels is

$$P_{sct}^m(k, n) = 1 - F_{sct}^m(k, n)\beta_k(\alpha) = 1 - (F_{sct}^m(k, 2))^{n-1}\beta_k(\alpha). \quad (17)$$

Between transmissions, there are idle times used for transient time-settling. Let the data occupancy ratio at the last slot for a k -slot packet be

$$\hat{r}_1 = 366/625, \hat{r}_3 = 372/625, \hat{r}_5 = 370/625. \quad (18)$$

For simplicity, they are approximated by a single value \hat{r} , i.e., $\hat{r} = r_3$. Poisson traffic is assumed in the piconets, and λ_1, λ_3 and λ_5 are the arrival rates of one-, three-, and five-slot packets respectively. λ_{10} is the arrival rate of the idle (one-slot) packets. As given in [7], let $B_j, j = 1, \dots, 10$, be the delimiter of time slots, where B_1, B_2 , and B_5 are the beginnings of one-, three-, and five-slot packets, respectively; B_3 and B_4 are the beginnings of the second and third slots of a three-slot packet, respectively; B_6, B_7, B_8 , and B_9 are the beginnings of the second, third, fourth, and fifth slots of a five-slot packet, respectively; and B_{10} is the beginning of an empty slot. The arrival rate of B_j is λ_j , and

$$\lambda_2 = \lambda_3 = \lambda_4, \quad (19)$$

$$\lambda_5 = \lambda_6 = \lambda_7 = \lambda_8 = \lambda_9. \quad (20)$$

Given any $B_j, g(j)$ is defined as the number of slots that follow delimiter B_j and belong to the same packet. Therefore

$$g(1) = 1, g(2) = 3, g(3) = 2, g(4) = 1, g(5) = 5, \quad (21)$$

$$g(6) = 4, g(7) = 3, g(8) = 2, g(9) = 1, g(10) = 1. \quad (22)$$

It is shown in [7] that

$$F_{sct}^m(k, 2) = \sum_{j=1}^{10} \left\{ (1 - \hat{r})\lambda_j \left[\tilde{f}(j)L(k - g(j)) + f(k, j) \cdot \tilde{L}(k - g(j)) \right] + (2\hat{r} - 1)\lambda_j f(j)L(k - g(j)) \right\}, \quad (23)$$

where the following definitions are duplicated from [7]

$$\tilde{f}(j) = \begin{cases} 1 & \text{if } j = 10, \\ s_0 & \text{o.w.,} \end{cases} \quad (24)$$

$$f(j) = \begin{cases} \frac{(\lambda_1 + \lambda_3 + \lambda_5)s_0^2 + \lambda_{10}s_0}{\lambda_1 + \lambda_3 + \lambda_5 + \lambda_{10}} & j = 1, 2, 5, \\ \frac{(\lambda_1 + \lambda_3 + \lambda_5)s_0 + \lambda_{10}}{\lambda_1 + \lambda_3 + \lambda_5 + \lambda_{10}} & j = 10, \\ s_0 & \text{o.w.,} \end{cases} \quad (25)$$

$$f(k, j) = \begin{cases} \frac{(\lambda_1 + \lambda_3 + \lambda_5)s_0 + \lambda_{10}}{\lambda_1 + \lambda_3 + \lambda_5 + \lambda_{10}} & k = 1, j = 1, 2, 5, \\ \frac{(\lambda_1 + \lambda_3 + \lambda_5)s_0^2 + \lambda_{10}s_0}{\lambda_1 + \lambda_3 + \lambda_5 + \lambda_{10}} & k = 3, 5, j = 1, 2, 5, \\ \frac{(\lambda_1 + \lambda_3 + \lambda_5)s_0 + \lambda_{10}}{\lambda_1 + \lambda_3 + \lambda_5 + \lambda_{10}} & j = 10, \\ s_0 & \text{o.w.,} \end{cases} \quad (26)$$

$$L(i) = \frac{\lambda_{10}L(i - g(10))}{\lambda_1 + \lambda_3 + \lambda_5 + \lambda_{10}} + \frac{\lambda_1 s_0 L(i - g(1))}{\lambda_1 + \lambda_3 + \lambda_5 + \lambda_{10}} \\ + \frac{\lambda_3 s_0 L(i - g(2))}{\lambda_1 + \lambda_3 + \lambda_5 + \lambda_{10}} + \frac{\lambda_5 s_0 L(i - g(5))}{\lambda_1 + \lambda_3 + \lambda_5 + \lambda_{10}}, \quad (27)$$

for $i > 0$, and $L(i) = 1$ for $i \leq 0$, and

$$\tilde{L}(i) = \frac{\lambda_{10}\tilde{L}(i - g(10))}{\lambda_1 + \lambda_3 + \lambda_5 + \lambda_{10}} + \frac{\lambda_1 s_0 \tilde{L}(i - g(1))}{\lambda_1 + \lambda_3 + \lambda_5 + \lambda_{10}} \\ + \frac{\lambda_3 s_0 \tilde{L}(i - g(2))}{\lambda_1 + \lambda_3 + \lambda_5 + \lambda_{10}} + \frac{\lambda_5 s_0 \tilde{L}(i - g(5))}{\lambda_1 + \lambda_3 + \lambda_5 + \lambda_{10}}, \quad (28)$$

for $i > 1$, and $\tilde{L}(i) = 1$ for $i \leq 1$. s_0 is defined in (4). Note that compared to [7], here (25) and (26) are slightly modified to reflect the probabilities for different types of slots.

Notice that by expanding (23), it can be obtained that

$$F_{sct}^m(1, 2) = a_2 s_0^2 + a_1 s_0 + a_0, \quad (29)$$

where s_0^0 , s_0 , and s_0^2 are the probabilities of packet success when there are one, two, and three synchronized piconets with the same type packets coexist in ideal channel without noise, and a_0 , a_1 , a_2 are the corresponding parameters accounting for the effect of mixed types of multi-slot packets. Generalizing this result to n piconets, it can be obtained that

$$P_{sct}^m(k, n) = 1 - \sum_{j=0}^{\gamma_k(n-1)} \beta_k(\alpha) a_j^{\langle n > 1 \rangle} s_0^j = 1 - \sum_{j=0}^{\gamma_k(n-1)} a_j^{\langle n > 1 \rangle} (1 - P_{sct}^s(k, j + 1)), \quad (30)$$

where $k = 1, 3, 5$, $\gamma_1 = 2$, $\gamma_3 = 3$, $\gamma_5 = 5$, and $P_{sct}^s(k, j + 1)$ is defined in (4).

Similarly, for DCT, the PER for k -slot packets when n piconets with mixed packet types coexist in AWGN channels is

$$P_{dct}^m(k, n) = 1 - \sum_{j=0}^{\gamma_k(n-1)} a_j^{\langle n > 1 \rangle} (1 - P_{dct}^s(k, j + 1)), \quad (31)$$

where k , γ_k , a_j are defined in (30), and $P_{dct}^s(k, j + 1)$ is defined in (11).

The throughputs per piconet when n piconets coexist for SCT and DCT are

$$R_{sct}(n) = \lambda_1 (1 - P_{sct}^m(1, n)) r_1 + 3\lambda_3 (1 - P_{sct}^m(3, n)) r_3 + 5\lambda_5 (1 - P_{sct}^m(5, n)) r_5 \text{ Mbps}, \quad (32)$$

$$R_{dct}(n) = \lambda_1 (1 - P_{dct}^m(1, n)) r_1 + 3\lambda_3 (1 - P_{dct}^m(3, n)) r_3 + 5\lambda_5 (1 - P_{dct}^m(5, n)) r_5 \text{ Mbps}. \quad (33)$$

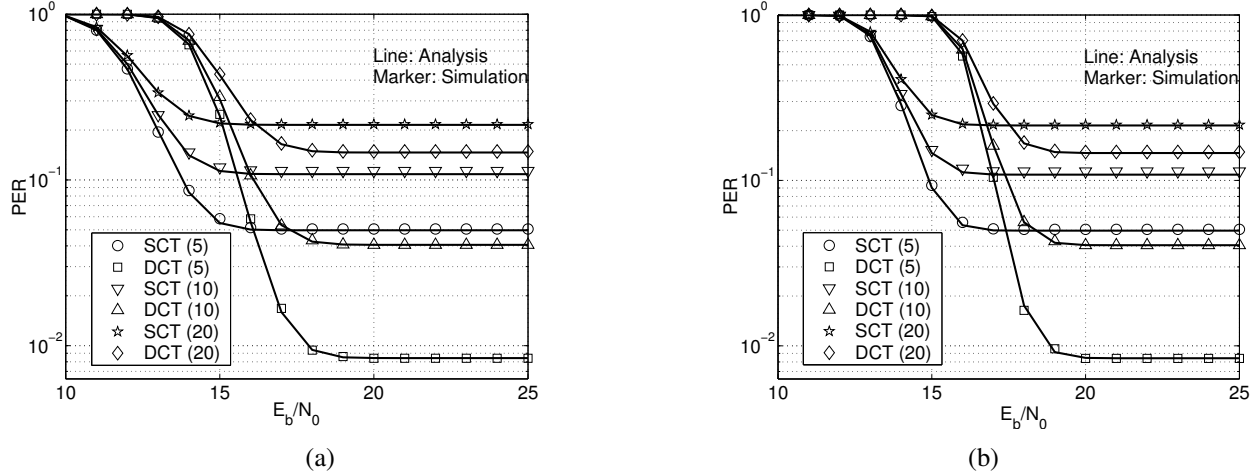


Figure 6: PER for versus E_b/N_0 : (a) one-slot packet; (b) five-slot packet.

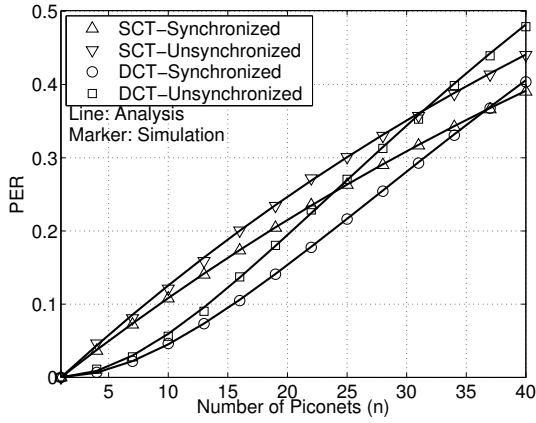
E.1.3 Simulations and Discussion

Monte-Carlo simulations are used to validate the theoretical analysis. The performance for DCT with two channels separated by at least $D = 22$ MHz is evaluated. Each channel uses half the power that would be used in SCT. AWGN channel is simulated. Fig. 6 depicts the PER for synchronized piconets versus SNR when the number of piconets is 5, 10, and 20. The results for piconets with one-slot and five-slot packets are shown. The results for piconets with three-slot packets will fall within the range of the aforementioned two cases and are omitted here. In Fig. 6, “DCT (10)” means that 10 synchronized piconets with DCT coexist. Since the signal power for each channel of DCT is only half of what would be used in SCT, DCT outperforms SCT only when PER is dominated by collisions, which is the case when SNR is greater than 18 dB for SCT (equivalently, 15 dB in each channel of DCT). The error floors in Fig. 6 indicate that when SNR is sufficient high, the noise effect on PER can be neglected.

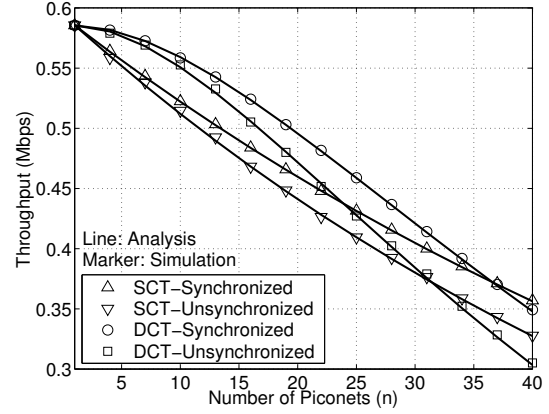
A Bluetooth transmitter has three levels of radio transmission power: 20 dBm, 4 dBm and 0 dBm. As shown in [32], considering 70 dB loss for a 10 m link, a noise level of -114 dBm at the receiver input, and a receiver noise figure 23 dB, a typical transmit power of 0 dBm in Bluetooth will result in a receive SNR of 21 dB. Therefore, Bluetooth typically operates in an SNR range where DCT outperforms SCT.

In Fig. 7, the PER and throughput per piconet are plotted for SCT and DCT as a function of the number of piconets. The average packet transmission time is shown in Fig. 8 (a). Synchronized and fully unsynchronized cases with one-slot packet are simulated. The results for three-slot and five-slot packets are similar to these results. The SNR is 18 dB, under which the effect of noise can be ignored compared to that of collisions. From these figures, it can be seen that the simulation results match well with the theoretic analysis. When the number of piconets is 10, for the synchronized case, the PERs for SCT and DCT are 11% and 4.3% respectively, the throughput per piconet for SCT and DCT are 0.5213 Mbps and 0.5605 Mbps respectively. Therefore, with DCT, the PER reduces by 61% and the throughput increases by 8% compared to SCT. From Fig. 8 (a), it is observed that DCT also outperforms SCT in term of average packet transmission time, so that DCT significantly outperforms SCT when the number of piconets is less than 30. Note that in a practical scenario, it is rare to have more than a dozen co-located piconets due to the short transmission distance of Bluetooth.

Figs. 6–8 (a) show that DCT outperforms SCT when the total number of piconets is less than 20. Naturally one may think to use triple or even more channels simultaneously to transmit a packet in order

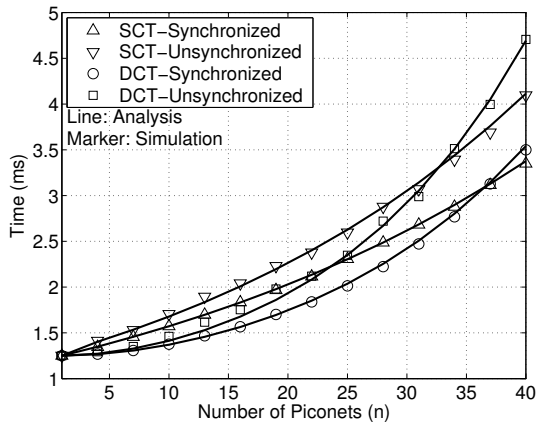


(a)

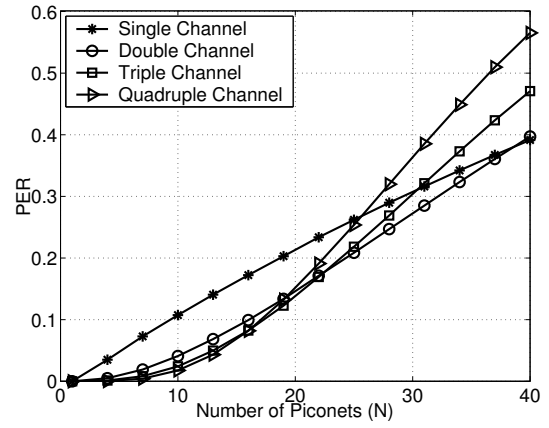


(b)

Figure 7: Performance for piconet with one-slot packet: (a) PER; (b) throughput.

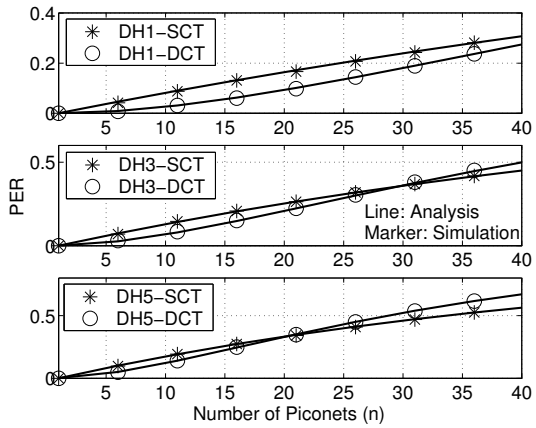


(a)

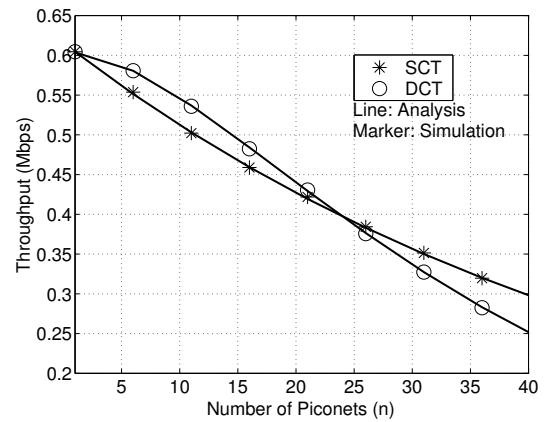


(b)

Figure 8: (a) Average packet transmission time. (b) PER for frequency diversity methods on different number of channels.



(a)



(b)

Figure 9: Performance for mixed packet type case: (a) PER; (b) throughput.

to further reduce PER. However, due to more frequency channels used, there are also more collisions. Assuming channels are distinct, the PER is obtained for multiple channel transmissions using simulations. The results for SCT, DCT, triple channel transmission (TCT), and quadruple channel transmission (QCT) are shown in Fig. 8 (b), where it is assumed that all piconets transmit synchronized one-slot packets and the SNR is infinity. It can be seen that further PER reduction over DCT by using TCT or QCT is marginal, compared to the improvement provided by DCT over SCT. Considering the balance of complexity and performance, DCT is the preferred choice.

Next, piconets with mixed packet types are considered. The PERs for different data packets (DH_i means i -slot packet) and throughput per piconet are plotted in Fig. 9 for SCT and DCT. The SNR is 18 dB. The arrival rates $\lambda_1 = \lambda_3 = \lambda_5$, and the traffic load is 70%. Compared to SCT, DCT reduces PER by as much as 50% and increases throughput by up to 6%, when the number of piconets is small (less than 20).

E.2 Coexistence of Multiple Bluetooth Piconets and a WLAN

E.2.1 Performance Analysis

In this section, the performance of DCT when there are multiple Bluetooth piconets co-located with a WLAN is evaluated. A hop frequency falling into the 22 MHz WLAN band results in a collision in that channel. The performance of the proposed DCT is compared to those of SCT and AFH. For simplicity, only the PER for synchronized Bluetooth piconets with the same type packets in this section is considered. The other cases can be analyzed using a similar method.

A packet from a piconet with SCT is successfully received only when no bit error occurs due to noise or collision, where the collision can happen between Bluetooth piconets or between the Bluetooth piconet and WLAN. The PER for n synchronized piconets with SCT, when co-located with a WLAN in AWGN channels, is given by

$$P_{sct}^w(k, n) = 1 - s_0^{n-1} \beta_k(\alpha) \gamma, \quad (34)$$

where the superscript w in $P_{sct}^w(k, n)$ stands for the case that multiple Bluetooth piconets coexist with a WLAN. $\gamma = (M - D)/M$ denotes the probability that a Bluetooth frequency falls outside the WLAN band.

Then, the PER performance of AFH is analyzed. Suppose that after an initial time period, the AFH scheme successfully detects the D MHz band occupied by a WLAN, and subsequently avoids hopping onto this band. The probability that one interfering piconet chooses another frequency instead of the one chosen by the piconet of interest is

$$\tilde{s}_0 = (M - 1 - D)/(M - D). \quad (35)$$

With AFH, a packet is successfully received only when no bit error occurs due to noise or collision between Bluetooth piconets. The PER for n synchronized piconets with AFH, when co-located with a WLAN in AWGN channels is

$$P_{afh}^w(k, n) = 1 - \tilde{s}_0^{n-1} \beta_k(\alpha). \quad (36)$$

Similar to the SCT case, by revising (11), the PER for n synchronized Bluetooth piconets with DCT,

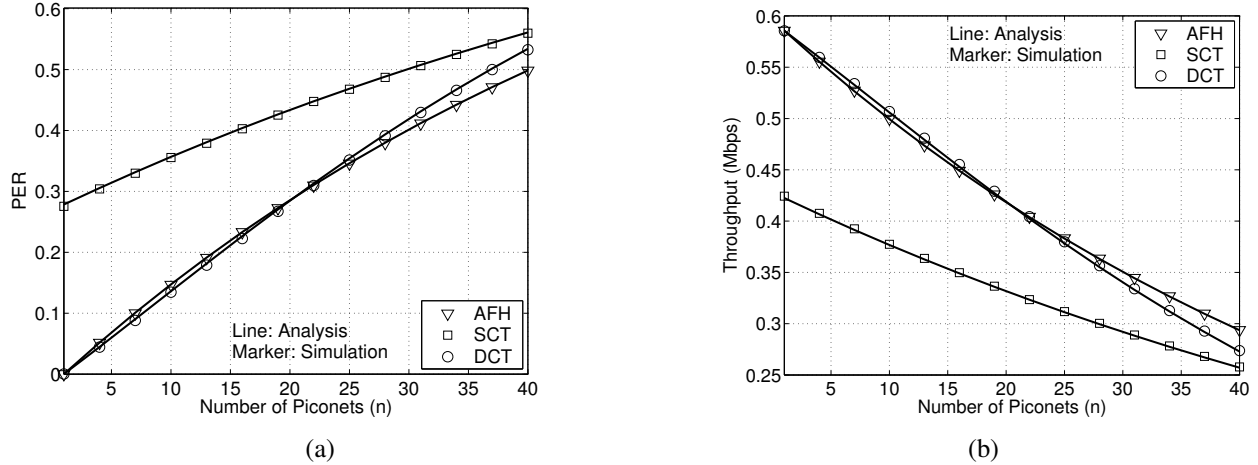


Figure 10: Performance when coexist with a WLAN: (a) PER; (b) throughput.

when co-located with a WLAN in AWGN channels, can be obtained as

$$\begin{aligned}
 P_{dct}^w(k, n) = & 1 - \sum_{i=0}^{n-1} 2^i \binom{n-1}{i} d_0^{n-1-i} d_1^{\langle i>0} (d_2^{i-1})^{\langle i>1} \\
 & \cdot [1 - (1 - \beta_k(\alpha/2))^2]^{\langle i=0 \rangle} \beta_k(\alpha/2)^{\langle i>0} \gamma^{\langle i>0}.
 \end{aligned} \tag{37}$$

E.2.2 Simulations and Discussion

Fig. 10 shows the PERs for SCT, AFH, and DCT as functions of the number of piconets when multiple Bluetooth piconets coexist with a WLAN. It is assumed that all piconets are synchronized and they transmit single-slot packets. In each realization of the Monte-Carlo simulation, the center frequency of the WLAN band is randomly generated among the eleven channels for 802.11b WLAN as listed in table I of [18]. In addition, it is assumed that for Bluetooth with AFH, the band occupied by the WLAN is already known, therefore AFH is able to avoid hopping onto the WLAN band. From Fig. 10, it can be observed that DCT has performance comparable to that of AFH when the total number of Bluetooth piconets is small, and both outperform SCT significantly. In practice, if the channel status changes, the master device in a Bluetooth piconet with AFH has to communicate with each slave device to update the frequency classification information, which reduces the total useful throughput. In contrast, DCT works independently and does not require an initial period to detect the WLAN band, and it is robust to both dynamic and static interference.

E.3 Performance in Realistic Scenario

As shown in [33], the effect of adjacent channel interference on the BER can not be neglected. A semi-analytical approach is developed in [34] to evaluate the performance of Bluetooth transmission considering the geometry of the environment. In this case, a frequency collision will not necessarily destroy a packet, if the power of the interfering signal at the receiver is not high enough. In order to present a more accurate analysis, in this section, the performance of SCT and DCT in more realistic scenario is analyzed. Different from [34], not only the geometry of the environment, the position of the reference receiver (RR) and the propagation characteristics, e.g., path loss and shadowing, but also the adjacent channel interference are considered.

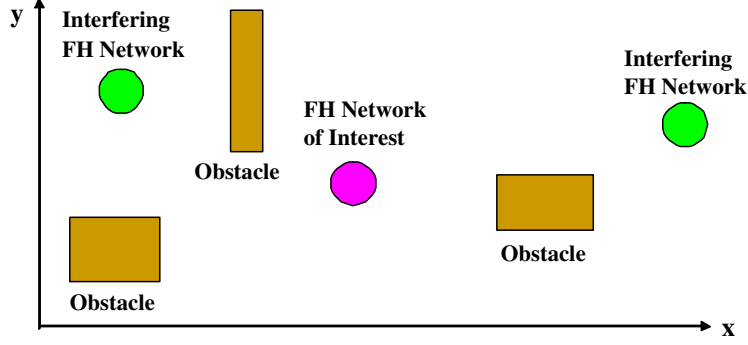


Figure 11: An example geometrical arrangement in the local area.

E.3.1 Performance Analysis

From the analysis of Section E.1, it is assumed that SNR is sufficient high (≥ 18 dB in SCT) and neglect the noise effect. Here all piconets are supposed to be synchronized. The geometrical arrangement is shown in Fig. 11. The transmitters of interfering piconets are located randomly with a uniform distribution in the square piconet area and the transmitter of the piconet of interest is located randomly with a uniform distribution in the round coverage area of the RR. For comparison, the performance for both SCT and DCT is analyzed.

PER of SCT

First of all, $W_T^s = 1$ mW is defined as the transmitted power at a Bluetooth device, W_R^s is defined as the power received by the reference receiver, and U_i^s is defined as the interference power in the RR due to interfering piconet i . The superscript s stands for SCT. The interfering powers $U_i^s, i = 1, \dots, n-1$, depend on the propagation losses due to the transmitter-receiver distance and the geometry of the obstacles, which is modelled as

$$U_i^s = W_T^s \cdot 10^{-\Lambda(L_i)/10} \cdot S_i, \quad i = 1, \dots, n-1, \quad (38)$$

where the path loss $\Lambda(L_i)$ in dB is

$$\Lambda(L_i) = \begin{cases} 40 + 20 \log L_i, & L_i \leq 8.5 \\ 25.3 + 36 \log L_i, & L_i > 8.5 \end{cases} \quad (39)$$

and the distance L_i is in meters. S_i is the shadowing factor and $10 \cdot \log S_i \sim N(0, \sigma^2)$, i.e., an unbiased Gaussian random variable in dB with a variance σ^2 .

Taking into account both co-channel and adjacent channel interference, in this case a packet error occurs when the ratio of the received carrier power to the sum of the normalized interference power is lower than 1 [35], so the PER for n synchronized piconets is

$$P'_{sct}(n) = \text{Prob} \left\{ \frac{W_R^s}{\sum_{i=1}^{n-1} \chi_i^s U_i^s} \leq 1 \right\} = \int_{-\infty}^0 f_{Z_{n-1}}(x) dx,$$

where $f_{Z_{n-1}}(x)$ is the probability density function (pdf) of

$$Z_{n-1} = W_R^s - \sum_{i=1}^{n-1} \chi_i^s U_i^s, \quad (40)$$

and $\chi_i^s, i = 1, \dots, n-1$, are independent, identically distributed random variables accounting for the normalization parameters of the interference.

χ_i^s is modelled as

$$\chi_i^s = \begin{cases} \gamma_0 & \text{with prob. } p_0 \text{ (co-channel interference)} \\ \gamma_1 & \text{with prob. } p_1 \text{ (adjacent channel interference)} \\ 0 & \text{with prob. } q = 1 - p_0 - p_1 \end{cases}$$

where the coefficients $\gamma_0 = 10^{1.1}$ and $\gamma_1 = 1$. These factors represent the required signal-to-interference ratio to achieve an uncoded BER of 0.1%. Similar to [34], a packet error occurs when BER is greater than 0.1%. According to Table 4.1 of the Bluetooth specification [3], the BER shall be less than 0.1% if the signal-to-interference ratio is greater than 11 dB for co-channel interference, or greater than 0 dB for adjacent 1 MHz interference, or greater than -30 dB for adjacent 2 MHz interference. Here, only the most significant interferences are considered, they are the co-channel interference and the adjacent 1 MHz interference. Therefore $\gamma_0 = 10^{1.1}$ and $\gamma_1 = 1$. As shown in [33], the probability that a frequency from an interfering piconet hops into the frequency channel of the piconet of interest is $p_0 = 1/M$, and the probability that it hops into the adjacent channels is $p_1 = 2(M-1)/M^2$.

The pdf of Z_{n-1} is

$$f_{Z_{n-1}}(x) = f_{W_R^s}(x) * f_1(-x) * \dots * f_{n-1}(-x), \quad (41)$$

where $*$ denotes convolution, $f_{Z_0}(x) = f_{W_R^s}(x)$, and $f_i(x)$ is defined as

$$f_i(x) = q\delta(x) + \frac{p_0}{\gamma_0} f_{U^s}\left(\frac{x}{\gamma_0}\right) + \frac{p_1}{\gamma_1} f_{U^s}\left(\frac{x}{\gamma_1}\right), \quad (42)$$

for $i = 1, \dots, n-1$, where $\delta(x)$ is the Dirac delta function. Since the signal transmitted by each interfering piconet goes through the same propagation environment, it is assumed that the statistics of the interfering power is independent of the index i , so U^s instead of U_i^s is used in (42).

By integrating (41) over $(-\infty, 0)$, the PER is obtained as

$$P'_{sct}(n) = \sum_{i=0}^{n-1} \sum_{j=0}^{n-1-i} \binom{n-1}{i} \binom{n-1-i}{j} q^{n-1-i-j} p_0^i p_1^j \beta_{i,j}^d, \quad (43)$$

where

$$\beta_{i,j}^s = \int_{-\infty}^0 g_i(x) * g_j(x) * f_{W_R^s}(x) dx, \quad (44)$$

and

$$g_i(x) = \gamma_0^{-i} \underbrace{f_{U^s}(-x/\gamma_0) * \dots * f_{U^s}(-x/\gamma_0)}_{\text{total } i \text{ } f_{U^s}(-x/\gamma_0)}, \quad (45)$$

$$g_j(x) = \gamma_1^{-j} \underbrace{f_{U^s}(-x/\gamma_1) * \dots * f_{U^s}(-x/\gamma_1)}_{\text{total } j \text{ } f_{U^s}(-x/\gamma_1)}, \quad (46)$$

and $g_0(x) = \delta(x)$. Since

$$\int_{-\infty}^0 f_{W_R^s}(x) dx = 0, \quad (47)$$

$\beta_{0,0}^s = 0$. The term $\binom{n-1}{i} \binom{n-1-i}{j} q^{n-1-i-j} p_0^i p_1^j$ is the probability that among $n-1$ interfering piconets, i interfering piconets are transmitting on the same channel of the piconet of interest, and j interfering piconets

are transmitting on the adjacent channels of the piconet of interest. The coefficient $\beta_{i,j}^s$ accounts for the PER reduction due to the environment propagation characteristics, e.g., path loss and shadowing. $\beta_{i,j}^s$ is always less than unity and it approaches unity when i, j become bigger.

The overall propagation loss depends on the position of the piconets. Since all the signals undergo the same propagation environment, the statistical approximations for the pdfs of $f_{U^s}(x)$ and $f_{W_R^s}$ are obtained from a spatial discretization of the network area using the method in [34]. The interfering power U^s is approximated over the whole network area as a discrete random variable assuming a finite set of discrete values $\Pi_1, \Pi_2, \dots, \Pi_K$ with probabilities $\pi_1, \pi_2, \dots, \pi_K$ respectively, i.e.,

$$f_{U^s} = \sum_{k=1}^K \pi_k \delta(x - \Pi_k), \quad (48)$$

where K is the total number of power intervals. The pdf of the received useful power is obtained following the same approach except that it is based on the coverage area of the RR.

PER of DCT

Since half the power is used in each channel of DCT, $W_T^d = W_T^s/2 = 0.5$ mW is defined as each channel's transmitted power for piconets with DCT. W_R^d is defined as the power received by the reference receiver for each channel, and U_i^d is defined as the power received at the RR from one channel of the interfering piconet i . The superscript d stands for DCT. The path loss model used for each channel of DCT is the same as that of SCT. If considering the propagation characteristics, a packet error in DCT occurs only if the ratios of the received carrier power to the sum of the normalized interference power in both channels are less than 1:

$$P'_{dct}(n) = \text{Prob} \left\{ \frac{W_R^d}{\sum_{i=1}^{n-1} \chi_{i,1}^d U_i^d} \leq 1, \frac{W_R^d}{\sum_{i=1}^{n-1} \chi_{i,2}^d U_i^d} \leq 1 \right\},$$

where $\chi_{i,1}^d, \chi_{i,2}^d, i = 1, \dots, n-1$, account for the normalization parameters for the interference. The subscript $i,1$ and $i,2$ denote that the two channels of the piconet of interest are affected by the interference from piconet i .

$\chi_{i,1}^d$ and $\chi_{i,2}^d$ are modelled as $\chi_{i,1}^d = \gamma_s$ and $\chi_{i,2}^d = \gamma_t$ with probability $z_{s,t}$ for $s, t = 0, 1, 2$, where $\gamma_0 = 10^{1.1}$, $\gamma_1 = 1$ and $\gamma_2 = 0$. Suppose that piconet A is the piconet of interest and piconet B is the interfering piconet. $s = 0, 1, 2$ denote that one channel of A suffers co-channel interference, adjacent interference or no interference from B , respectively. $t = 0, 1, 2$ denote that the other channel of A suffers co-channel interference, adjacent interference or no interference from B , respectively. For example, $z_{0,1}$ denotes the probability that one channel of B is co-channel interference and the other channel of B is adjacent interference to A . This probability is calculated as

$$z_{0,1} = \sum_{i=1}^M \sum_{j=1}^M \left[\frac{T_j}{M} \left(\frac{T_{i-1} + T_{i+1} + T_{j-1} + T_{j+1}}{M} + \frac{4T_i}{M} \right) \right],$$

where T_j/M is the average probability for $a_1 = i$ and $a_2 = j$, a_1 and a_2 are the channels of piconet A . In addition, $(T_{i-1} + T_{i+1} + T_{j-1} + T_{j+1})/M$ is the probability that b_1 is equal to a_1 , and b_2 is equal to $a_1 - 1, a_1 + 1, a_2 - 1, \text{ or } a_2 + 1$. $4T_i/M$ is the probability that b_2 is equal to a_1 , and b_1 is equal to $a_1 - 1, a_1 + 1, a_2 - 1, \text{ or } a_2 + 1$.

When two piconets with DCT coexist, the PER is

$$\begin{aligned}
P'_{dct}(2) &= \beta_{1,0}^d \beta_{1,0}^d z_{0,0} + \beta_{1,0}^d \beta_{0,1}^d z_{0,1} + \beta_{1,0}^d \beta_{0,0}^d z_{0,2} \\
&+ \beta_{0,1}^d \beta_{1,0}^d z_{1,0} + \beta_{0,1}^d \beta_{0,1}^d z_{1,1} + \beta_{0,1}^d \beta_{0,0}^d z_{1,2} \\
&+ \beta_{0,0}^d \beta_{1,0}^d z_{2,0} + \beta_{0,0}^d \beta_{0,1}^d z_{2,1} + \beta_{0,0}^d \beta_{0,0}^d z_{2,2},
\end{aligned} \tag{49}$$

where $\beta_{i,j}^d$ is defined as in (44) except that the transmission power for each channel of both the interfering piconet and the piconet of interest is decreased by half.

Generalizing (49), the PER for n piconets is obtained as

$$\begin{aligned}
P'_{dct}(n) &= \sum_{i=0}^{e_1} \sum_{j=0}^{e_2} \sum_{k=0}^{e_3} \sum_{r=0}^{e_4} \sum_{s=0}^{e_5} \sum_{t=0}^{e_6} \sum_{u=0}^{e_7} \sum_{v=0}^{e_8} \binom{e_1}{i} \binom{e_2}{j} \binom{e_3}{k} \binom{e_4}{r} \binom{e_5}{s} \\
&\times \binom{e_6}{t} \binom{e_7}{u} \binom{e_8}{v} z_{0,0}^i z_{0,1}^j z_{0,2}^k z_{1,0}^r z_{1,1}^s z_{1,2}^t z_{2,0}^u z_{2,1}^v z_{2,2}^{e_8-v} \\
&\times \beta_{i+j+k,r+s+t}^d \beta_{i+r+u,j+s+v}^d,
\end{aligned} \tag{50}$$

where $e_1 = n - 1$, $e_2 = e_1 - i$, $e_3 = e_2 - j$, $e_4 = e_3 - k$, $e_5 = e_4 - r$, $e_6 = e_5 - s$, $e_7 = e_6 - t$, $e_8 = e_7 - u$. $\beta_{i+j+k,r+s+t}^d$ accounts for the PER reduction due to the propagation attenuation for one channel of piconet A . $\beta_{i+r+u,j+s+v}^d$ accounts for the PER reduction due to the propagation attenuation for the other channel of A . The coefficient corresponding to each $\beta_{i+j+k,r+s+t}^d \beta_{i+r+u,j+s+v}^d$ is the probability that one channel of A suffers from $i + j + k$ co-channel interference and $r + s + t$ adjacent channel interference, the other channel of A suffers from $i + r + u$ co-channel interference and $j + s + v$ adjacent channel interference.

E.3.2 Simulations and Discussion

Monte-Carlo simulations are used to validate the theoretic analysis. All piconets are assumed to be synchronized. Fig. 12 shows the PER and throughput for SCT and DCT as functions of the number of piconets when multiple Bluetooth piconets coexist, where co-channel and adjacent channel interference as well as propagation characteristics are considered. In each realization of the simulation, the position of each piconet is selected randomly in a $10\text{m} \times 10\text{m}$ area, the RR is located in the center. Here $\sigma = 4$ dB for shadowing. It can be seen from Fig. 12 that when the adjacent channel interference is considered, the performance degrades, but DCT still outperforms SCT when the total number of piconets is less than 20.

F A Single-Antenna Multi-Carrier Diversity Method

The analysis in Section E assumes an AWGN channel. However, high rate data transmission over radio channels also experiences signal corruption caused by multipath propagation. If the delay spread of the multipath dispersion exceeds the symbol period, symbols will be affected by ISI and the number of affected symbols grows linearly with the data rate. Then, the channel frequency response exhibits significant amplitude fluctuation over frequency, wireless channel with this characteristic is termed frequency-selective channel. Unlike Gaussian channel, frequency-selective channel suffers from attenuation due to destructive addition of multiple paths. Severe attenuation makes it impossible for the receiver to determine the transmitted signal unless a less-attenuated replica of the transmitted signal is provided to the receiver.

In this section, a novel single-antenna multi-carrier diversity technique with frequency hopped transmission over frequency-selective fading channels is developed. In order to take advantage of the frequency

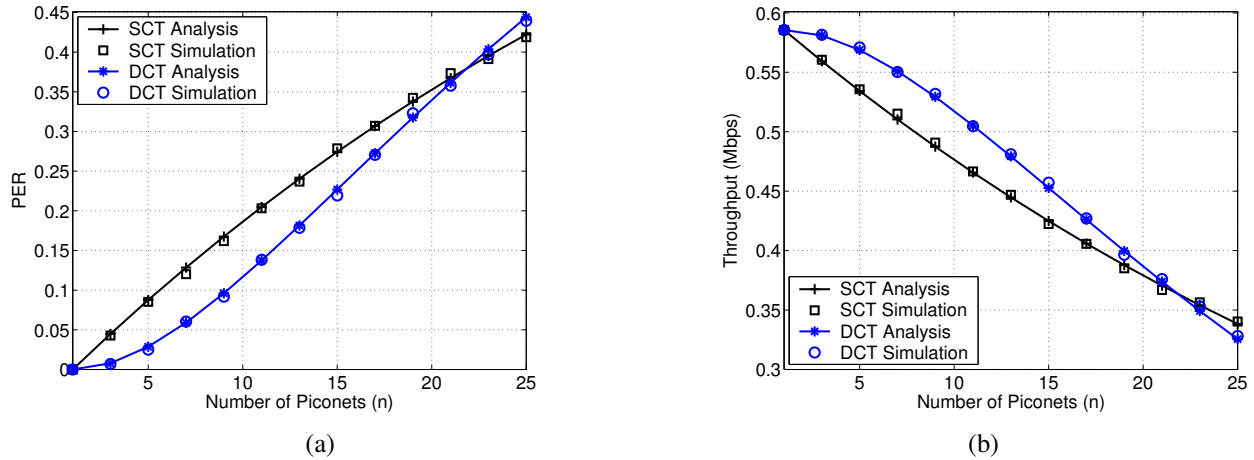


Figure 12: Performance in realistic case: (a) PER; (b) throughput.

diversity, the same symbol is transmitted on multiple carrier frequencies simultaneously. These carrier frequencies are distinct and randomly selected from the channel band. For each branch, the carrier frequency hops symbol by symbol. At the receiver, a selection or combining technique is applied on these branches. It is assumed that the channel state information (CSI) and the hop frequencies of these branches are known to the receiver. By evaluating the frequency response at the carrier frequencies, the receiver can choose to decode the one with the largest gain, or combine all of these signals, and thus the selection/combining diversity is collected. This technique can be easily applied to the DCT design proposed in Section E.

In high speed digital communications, the orthogonal frequency division multiplexing (OFDM) technique [36] has been widely adopted. By executing inverse fast Fourier transform (IFFT) at the transmitter, and fast Fourier transform (FFT) at the receiver, OFDM converts an ISI channel into parallel ISI-free subchannels, with gains equal to the channel's frequency response on the FFT grid. To eliminate interblock interference and facilitate diagonalization of the channel matrix, a cyclic prefix (CP) of length no less than the channel order is inserted per block at the transmitter and discarded at the receiver [37]. When the channel has nulls close to or on the FFT grid, the symbols carried on the corresponding subchannels may be lost. Various coding techniques can be implemented to address this issue. For example, the CFC proposed in [38] can guarantee symbol detectability and achieve maximum channel diversity order with a single antenna at the transmitter and the receiver.

It is shown that the received signal for each branch in the proposed design exhibits similarity to OFDM, and CFC can also be used for each branch to guarantee symbol detectability and achieve maximum channel diversity order. The advantage of the proposed technique is that no CP is required and better performance is achieved compared to CFC-OFDM. However, the proposed technique has strict requirements on bandpass filters to guarantee the performance, and it has a spectral efficiency loss since the same symbol is transmitted over multiple subcarriers simultaneously.

F.1 System Model

F.1.1 The Channel Model

A frequency-selective channel of order L is modeled as

$$\mathbf{h} = [h(0) \quad h(1) \quad \cdots \quad h(L)], \quad (51)$$

where L is the maximum delay spread in terms of the symbol period. Each tap is generated as an independent and identically distributed zero-mean complex Gaussian random variable so that its envelop obeys a Rayleigh distribution. Given (51), the channel impulse response can be written as

$$\bar{h}(t) = \frac{1}{\sqrt{L+1}} \sum_{l=0}^L h(l)\delta(t-lT), \quad (52)$$

where the constant $\frac{1}{\sqrt{L+1}}$ is to make the average channel energy equal to one, and T is the symbol period. Taking the Fourier transform of $\bar{h}(t)$, the channel frequency response is obtained as

$$H(f) = \frac{1}{\sqrt{L+1}} \sum_{l=0}^L h(l)e^{-j2\pi lTf}. \quad (53)$$

F.1.2 The Multi-Carrier Diversity System

In this model, the baseband modulation is binary phase shift keying (BPSK). Extension to other modulation schemes can be obtained similarly. A single antenna is used at the transmitter and the receiver. Without loss of generality, it is assumed that each symbol is transmitted on two carrier frequencies. The available channel band is split into M frequency bands and two distinct frequencies are randomly selected from them as the carrier frequencies. Let b_i ($i = 1, 2, \dots$) be the information bits. The narrow-band signal transmitted on the first branch is

$$\begin{aligned} s_1(t) &= \text{Re} \left\{ \beta^{\text{MC}} s_i e^{j2\pi f_{i,1}t} \right\} \\ &= \text{Re} \left\{ \beta^{\text{MC}} \sqrt{E_s} e^{j\theta_i} e^{j2\pi f_{i,1}t} \right\} \\ &= \beta^{\text{MC}} \sqrt{E_s} \cos(2\pi f_{i,1}t + \theta_i), \end{aligned} \quad (54)$$

for $0 \leq t \leq T$, $f_{i,1}$ is the carrier frequency for the i th symbol of the first branch. In (54), $s_i = \sqrt{E_s} e^{j\theta_i}$ is the BPSK symbol with $\theta_i = 2\pi(b_i - 1)/B$, $B = 2$ and E_s is the symbol energy. β^{MC} is the power loss factor, which is used to keep the total transmitted power the same even if multiple carriers are used. Here β^{MC} is equal to $1/\sqrt{2}$ because two channels are used.

The received signal is related to the input signal $s_1(t)$ and the channel response $\bar{h}(t)$ as

$$r_1(t) = \bar{h}(t) * s_1(t). \quad (55)$$

By taking Fourier transform of the right side of (55), it can be obtained that

$$\begin{aligned} H(f)S_1(f) &= \beta^{\text{MC}} \sqrt{E_s} |H(f_{i,1})| \left[\cos(\theta_i + \alpha_{i,1}) \left(\frac{1}{2}\delta(f - f_{i,1}) + \frac{1}{2}\delta(f + f_{i,1}) \right) \right. \\ &\quad \left. - \sin(\theta_i + \alpha_{i,1}) \left(\frac{1}{2j}\delta(f - f_{i,1}) - \frac{1}{2j}\delta(f + f_{i,1}) \right) \right], \end{aligned} \quad (56)$$

where $S_1(f)$ is the spectrum of $s_1(t)$, and $H(f_{i,1}) = |H(f_{i,1})|e^{j\alpha_{i,1}}$ is the channel frequency response at $f = f_{i,1}$. Next, the inverse Fourier transform of (56) is taken to obtain

$$\begin{aligned} r_1(t) &= \beta^{\text{MC}} \sqrt{E_s} |H(f_{i,1})| [\cos(2\pi f_{i,1}t) \cos(\theta_i + \alpha_{i,1}) - \sin(2\pi f_{i,1}t) \sin(\theta_i + \alpha_{i,1})] \\ &= \beta^{\text{MC}} \sqrt{E_s} |H(f_{i,1})| \cos(2\pi f_{i,1}t + \theta_i + \alpha_{i,1}) \\ &= \beta^{\text{MC}} \sqrt{E_s} \text{Re} \{ H(f_{i,1}) e^{j\theta_i} e^{j2\pi f_{i,1}t} \}. \end{aligned} \quad (57)$$

Finally, by removing the carrier and considering also AWGN effect, the received baseband signal is obtained as

$$r_{i,1} = \beta^{\text{MC}} H(f_{i,1}) s_i + \eta_{i,1}, \quad (58)$$

where $\eta_{i,1}$ is the band limited noise for the i th symbol of the first branch. Similarly, the received baseband signal for the second branch is

$$r_{i,2} = \beta^{\text{MC}} H(f_{i,2}) s_i + \eta_{i,2}. \quad (59)$$

Since the CSI and the two carrier frequencies are assumed to be known to the receiver, $H(f_{i,1})$ and $H(f_{i,2})$ can be calculated. By comparing these values, the receiver can choose to decode the signal at a carrier frequency with a larger gain or combine these two signals together. Note that here the one with a larger SNR is not chosen because for practical implementations with high data rate, instantaneous noise level measurement may be difficult or expensive. The multi-carrier selection method is denoted as MCS and the multi-carrier combining method is denoted as MCC. Suppose $|H(f_{i,1})| > |H(f_{i,2})|$, by using selection diversity method, the i th received signal is

$$\tilde{s}_i^{\text{MCS}} = H^*(f_{i,1}) r_{i,1} = \beta^{\text{MC}} |H(f_{i,1})|^2 s_i + H^*(f_{i,1}) \eta_{i,1}. \quad (60)$$

The maximum likelihood estimation of s_i is

$$\hat{s}_i^{\text{MCS}} = \arg \min_{s_i} \|\tilde{s}_i^{\text{MCS}} - \beta^{\text{MC}} |H(f_{i,1})|^2 s_i\|. \quad (61)$$

For MCC, by applying combining technique, the i th received signal is

$$\begin{aligned} \tilde{s}_i^{\text{MCC}} &= H^*(f_{i,1}) r_{i,1} + H^*(f_{i,2}) r_{i,2} \\ &= (|H(f_{i,1})|^2 + |H(f_{i,2})|^2) \beta^{\text{MC}} s_i + H^*(f_{i,1}) \eta_{i,1} + H^*(f_{i,2}) \eta_{i,2}. \end{aligned} \quad (62)$$

The maximum likelihood estimation of s_i is

$$\hat{s}_i^{\text{MCC}} = \arg \min_{s_i} \|\tilde{s}_i^{\text{MCC}} - \beta^{\text{MC}} (|H(f_{i,1})|^2 + |H(f_{i,2})|^2) s_i\|. \quad (63)$$

F.1.3 Complex-Field Coding for Channel Diversity

In order to achieve better performance, the CFC proposed in [38] to enable the channel diversity is adopted. The system block diagram for the MCS method with two channels is shown in Fig. 13. First, each consecutive K transmitted symbols is grouped into blocks as \mathbf{s}_k , then it is multiplied with an $N \times K$ matrix $\Theta \in \mathbb{C}^{N \times K}$ (the encoder) to obtain

$$\mathbf{u}_k = \Theta \mathbf{s}_k, \quad (64)$$

where $\mathbf{u}_k \in \mathbb{C}^{N \times 1}$, $\mathbf{s}_k \in \mathbb{C}^{K \times 1}$ and $N \geq K + L$. Finally, symbols in \mathbf{u}_k are transmitted on multiple carriers as discussed in Section F.1.2. By encoding a length- K vector to a length- N vector, some redundancy is introduced so that the data rate is K/N . The encoder is designed to guarantee detectability and achieve maximum channel diversity order when ML decoder is adopted [38]. Since the encoder does not depend on the block index k , from now on the block index k will be dropped for brevity.

The CFC for the MCS method with two channels is introduced first. In Fig. 13, $\mathbf{f}_i = [f_{0,i}, \dots, f_{N-1,i}]^T$, $i = 1, 2$, denote the frequencies used in the two channels. Let f_n^{max} be the carrier frequency that $|H(f_n^{\text{max}})| =$

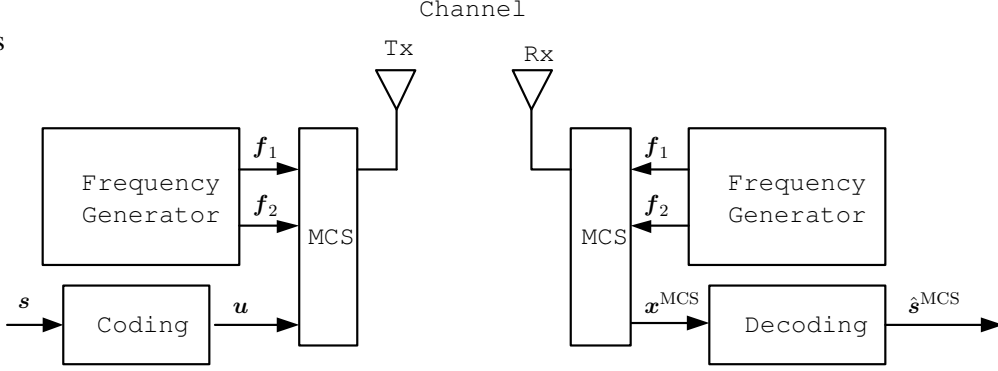


Figure 13: The system block diagram for MCS method with two channels.

$\max\{|H(f_{n,1})|, |H(f_{n,2})|\}$ for the n -th symbol in each block ($n = 0, 1, \dots, N-1$), the discrete-time baseband model can be described in vector form as

$$\mathbf{x}^{\text{MCS}} = \beta^{\text{MC}} \mathbf{D}^{\text{MCS}} \mathbf{u} + \boldsymbol{\eta} = \beta^{\text{MC}} \mathbf{D}^{\text{MCS}} \boldsymbol{\Theta} \mathbf{s} + \boldsymbol{\eta}, \quad (65)$$

where $\boldsymbol{\eta}$ is the band-limited noise vector with each item corresponding to the selected branch, and

$$\mathbf{D}^{\text{MCS}} = \text{diag}\left[H(f_0^{\text{max}}), H(f_1^{\text{max}}), \dots, H(f_{N-1}^{\text{max}})\right], \quad (66)$$

whose diagonal items are chosen from

$$\mathbf{D}_1 = \text{diag}\left[H(f_{0,1}), H(f_{1,1}), \dots, H(f_{N-1,1})\right], \quad (67)$$

$$\mathbf{D}_2 = \text{diag}\left[H(f_{0,2}), H(f_{1,2}), \dots, H(f_{N-1,2})\right]. \quad (68)$$

The maximum likelihood decoder can be formulated as follows:

$$\hat{\mathbf{s}}^{\text{MCS}} = \arg \min_{\mathbf{s}} \|\mathbf{x}^{\text{MCS}} - \beta^{\text{MC}} \mathbf{D}^{\text{MCS}} \boldsymbol{\Theta} \mathbf{s}\|. \quad (69)$$

As shown in [38], the maximum likelihood decoding requires exhaustive search, whose complexity depends exponentially on the number of symbols in the block. Therefore, it is not suitable for large block size N and/or high signal constellation. Linear equalizers such as the zero-forcing (ZF) and minimum mean square error (MMSE) equalizers provide low-complexity alternatives. Since noise variance is assumed unknown here, MMSE is not adopted. By applying the ZF equalization, the following result is obtained as the estimate for the signal block

$$\hat{\mathbf{s}}^{\text{MCS}} = \mathbf{s} + (\beta^{\text{MC}} \mathbf{D}^{\text{MCS}} \boldsymbol{\Theta})^\dagger \boldsymbol{\eta}. \quad (70)$$

Notice that as shown in [39], the achievable diversity order is still guaranteed by using ZF equalizer.

Similarly, for the CFC-MCC method, the discrete-time baseband model can be described as

$$\begin{aligned} \mathbf{x}^{\text{MCC}} &= \mathbf{D}_1^H (\beta^{\text{MC}} \mathbf{D}_1 \mathbf{u} + \boldsymbol{\eta}_1) + \mathbf{D}_2^H (\beta^{\text{MC}} \mathbf{D}_2 \mathbf{u} + \boldsymbol{\eta}_2) \\ &= \beta^{\text{MC}} \mathbf{D}^{\text{MCC}} \boldsymbol{\Theta} \mathbf{s} + \mathbf{D}_1^H \boldsymbol{\eta}_1 + \mathbf{D}_2^H \boldsymbol{\eta}_2, \end{aligned} \quad (71)$$

where $\mathbf{D}^{\text{MCC}} = \mathbf{D}_1^H \mathbf{D}_1 + \mathbf{D}_2^H \mathbf{D}_2$. By applying the ZF equalization, the following is obtained

$$\begin{aligned} \hat{\mathbf{s}}^{\text{MCC}} &= \mathbf{s} + [\beta^{\text{MC}} (\mathbf{D}_1^H \mathbf{D}_1 + \mathbf{D}_2^H \mathbf{D}_2) \boldsymbol{\Theta}]^\dagger (\mathbf{D}_1^H \boldsymbol{\eta}_1 + \mathbf{D}_2^H \boldsymbol{\eta}_2) \\ &= \mathbf{s} + (\beta^{\text{MC}} \mathbf{D}^{\text{MCC}} \boldsymbol{\Theta})^\dagger (\mathbf{D}_1^H \boldsymbol{\eta}_1 + \mathbf{D}_2^H \boldsymbol{\eta}_2), \end{aligned} \quad (72)$$

as the estimate for the signal block.

F.2 Performance Analysis

In this section, the performance of the proposed multi-carrier diversity technique is analyzed and compared to OFDM.

F.2.1 System Model for Uncoded/Coded OFDM

First, a brief review of the system model for CFC-OFDM is given. Here only the coded case is discussed. Note that if $K = N$ and Θ becomes an $N \times N$ identity matrix, the coded case will become the uncoded case. Suppose that the same coded symbol block $\mathbf{u} = \Theta \mathbf{s}$ as the one used in the proposed multi-carrier diversity technique is transmitted using OFDM. The IFFT is performed on \mathbf{u} to obtain $\tilde{\mathbf{u}} = \mathbf{F}^H \mathbf{u}$, where \mathbf{F} is the $N \times N$ FFT matrix with

$$[\mathbf{F}]_{n,v} = N^{-(1/2)} e^{-j2\pi nv/N}.$$

A CP of length L_{cp} is inserted in $\tilde{\mathbf{u}}$ to obtain $\bar{\mathbf{u}} = \beta^{\text{OFDM}} \mathbf{T}_{cp} \tilde{\mathbf{u}}$, where $\mathbf{T}_{cp} = [\mathbf{I}_{cp}^T \mathbf{I}_N^T]^T$ describes the CP insertion, \mathbf{I}_{cp} denotes the last L_{cp} rows of an $N \times N$ identity matrix \mathbf{I}_N . $\bar{\mathbf{u}}$ is a vector of length $N + L_{cp}$, $\beta^{\text{OFDM}} = \sqrt{N/(N + L_{cp})}$ is the power loss factor, which is used to maintain the same power. L_{cp} is chosen to be no less than L to eliminate ISI. Symbols in $\bar{\mathbf{u}}$ are then carrier modulated and transmitted sequentially.

After the carrier removal at the receiver, the received baseband signals are grouped into blocks of size $N + L_{cp}$ as $\bar{\mathbf{x}}$. Then, the first L_{cp} entries of $\bar{\mathbf{x}}$ corresponding to the CP are removed. Due to the CP insertion at the transmitter and CP removal at the receiver, the channel can be represented as an $N \times N$ circulant channel matrix:

$$[\tilde{\mathbf{H}}]_{n,v} = \frac{1}{\sqrt{L+1}} h((n-v) \bmod N), \quad (73)$$

where $h(\cdot)$ is the channel taps defined in (51). The signal at the receiver after CP removal is given by

$$\tilde{\mathbf{x}} = \beta^{\text{OFDM}} \tilde{\mathbf{H}} \tilde{\mathbf{u}} + \tilde{\boldsymbol{\eta}}, \quad (74)$$

where $\tilde{\boldsymbol{\eta}}$ is the AWGN noise vector. By applying FFT to $\tilde{\mathbf{x}}$, it is obtained that

$$\begin{aligned} \mathbf{x}^{\text{OFDM}} &= \beta^{\text{OFDM}} \mathbf{F} \tilde{\mathbf{H}} \tilde{\mathbf{u}} + \mathbf{F} \tilde{\boldsymbol{\eta}} \\ &= \beta^{\text{OFDM}} \mathbf{F} \tilde{\mathbf{H}} \mathbf{F}^H \mathbf{u} + \mathbf{F} \tilde{\boldsymbol{\eta}} \\ &= \beta^{\text{OFDM}} \mathbf{D}^{\text{OFDM}} \Theta \mathbf{s} + \mathbf{F} \tilde{\boldsymbol{\eta}}, \end{aligned} \quad (75)$$

where

$$\mathbf{D}^{\text{OFDM}} = \text{diag} \left[H(0), H\left(\frac{1}{N}\right), \dots, H\left(\frac{N-1}{N}\right) \right], \quad (76)$$

and $H(f)$ is the frequency response of the ISI channel as defined in (53) with $f = n/(NT)$ for $n = 0, 1, \dots, N-1$.

By applying the ZF equalization, the following is obtained

$$\hat{\mathbf{s}}^{\text{OFDM}} = \mathbf{s} + (\beta^{\text{OFDM}} \mathbf{D}^{\text{OFDM}} \Theta)^\dagger \mathbf{F} \tilde{\boldsymbol{\eta}}, \quad (77)$$

as the estimate for the OFDM signal block.

F.2.2 Comparison of MCS/MCC and OFDM for Uncoded Case

It is found that MCS method shows some similarity to the OFDM method. The input-output relationship in (65) for MCS and (75) for OFDM are considered for comparison. For the model structure, the similarities are that the same data vector is multiplied by a diagonal matrix. What is more, these diagonal matrices are similar to each other in that they all consist with channel frequency responses at certain frequencies. The matrix \mathbf{D}^{OFDM} can be considered as a special case of \mathbf{D}_1 (or \mathbf{D}_2) with $M = N$ frequencies sequentially and evenly selected from the subchannels. The differences are in three aspects. Firstly, each pair of carrier frequencies of MCS are randomly selected from M subchannels and the one with a larger gain is chosen to be present in \mathbf{D}^{MCS} . Secondly, their power loss factors are different. Thirdly, the noise vector of OFDM is FFT processed (note that the noise power spectrum density stays unchanged because the FFT is a norm-preserving linear transform), while the noise vector of MCS comes from narrow band noise.

The IFFT process and CP insertion and removal in OFDM are replaced by the frequency hopping technique in MCS and MCC. Without executing IFFT, the computation complexity is lower for MCS and MCC. But fast synchronization is required for MCS and MCC techniques. Since CP is not necessary for MCS and MCC, they achieve higher data rate than that of OFDM. For the uncoded case, MCS and MCC achieve full rate while OFDM has a rate of $N/(N + L_{cp})$. The block size N in OFDM should be greater than L and as big as possible to reach the higher rate. Since the computation complexity is $\mathcal{O}(N)$ for ZF and $\mathcal{O}(N \log N)$ for FFT [40], a bigger block size N implies higher computational complexity. The block size is variable for uncoded MCS and MCC.

Note that for the uncoded case, when the channel has nulls on or close to the carrier frequencies, \mathbf{D}^{OFDM} and \mathbf{D}_1 (or \mathbf{D}_2) will be ill-conditioned and serious noise amplification will emerge if they are inverted during the equalization step. In this case, the symbol transmitted on this carrier can not be recovered. Since the diagonal entries of \mathbf{D}^{OFDM} and \mathbf{D}_1 (or \mathbf{D}_2) represent frequency response samples of the channel \mathbf{h} evaluated at different frequencies, these diagonal entries are the linear combinations of the channel \mathbf{h} . Therefore, there can be at most L zeros on the diagonal of them. Then, the probability of having zeros on a diagonal entry of \mathbf{D}^{OFDM} or \mathbf{D}_1 (or \mathbf{D}_2) is at most L/N . By using two branches, the probability that \mathbf{D}^{MCS} or \mathbf{D}^{MCC} has nulls on its diagonal is at most $(L/N)^2$, which is much smaller than that for \mathbf{D}^{OFDM} . Note that by using more branches, further improvement may not always be achieved. Since the total power is kept constant, there is a tradeoff between the decreased power in each branch and the increased diversity by using more branches.

Here the average local signal-to-noise power ratio is evaluated for an M -branch selection system. Recall that each tap of the channel is assumed to have an envelop that obeys a Rayleigh distribution. Then, as seen from (53), the amplitude of $H(f)$ still obeys the Rayleigh distribution. As shown in [41], by assuming that both the transmitted signal power and the noise power are one, the local signal-to-noise power ratio γ_j for each branch at the receiver has a simple distribution

$$G(\gamma_j) = 1 - e^{-\gamma_j}. \quad (78)$$

Suppose that the largest power ratio is less than γ_{MCS} , then all branches have power ratio less than γ_{MCS} . Assuming that all branches are independent, the probability that all branches have power ratios less than γ_{MCS} is simply the product of each branch has a power ratio less than γ_{MCS} . The distribution function of the local power ratio γ_{MCS} for an M -order selection diversity system is

$$S_M(\gamma_{\text{MCS}}) = G(\gamma_{\text{MCS}})^M = (1 - e^{-\gamma_{\text{MCS}}})^M. \quad (79)$$

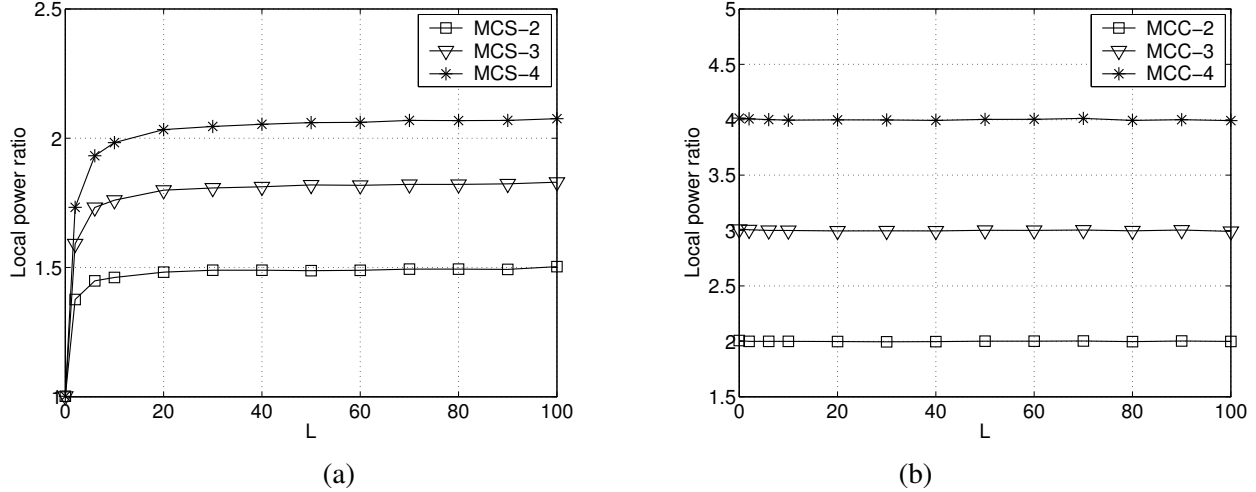


Figure 14: Local power ratio for: (a) the selection diversity system; (b) the combining diversity system.

The average value $\bar{\gamma}_{\text{MCS}}$ of γ_{MCS} is obtained as in [41]

$$\bar{\gamma}_{\text{MCS}}(M) = \int_{-\infty}^{\infty} \gamma_{\text{MCS}} dS_M(\gamma_{\text{MCS}}) = \sum_{j=1}^M \frac{1}{j}. \quad (80)$$

Therefore, $\bar{\gamma}_{\text{MCS}}(2) = 3/2$, $\bar{\gamma}_{\text{MCS}}(3) = 11/6$, $\bar{\gamma}_{\text{MCS}}(4) = 25/12$ and so on. Adding an extra M th branch increases $\bar{\gamma}_{\text{MCS}}$ by $1/M$.

The average local power ratio for $L = [0, 2, 6, 10, 20, \dots, 100]$ is shown in Fig. 14 (a) for dual branch selection (denoted as MCS-2), triple branch selection (denoted as MCS-3) and quad branch selection (denoted as MCS-4) techniques. From this figure, it can be found that when L becomes larger, the local power ratios approach $3/2$, $11/6$ and $25/12$ respectively. In spatial diversity systems, a certain antenna separation is required to mitigate correlation effects. While in the proposed selection diversity system, a large channel tap L can reduce the correlation between branches, due to the structure of (53). For example, when $L = 0$, the channel is frequency-flat and each two branches are fully correlated. In this case there is no selection diversity.

For an M -branch combining diversity system, the local power ratio γ_{MCC} is obtained in [41] as

$$\gamma_{\text{MCC}}(M) = \sum_{j=1}^M \gamma_j. \quad (81)$$

The average local power ratio $\bar{\gamma}_{\text{MCC}}$ is given by

$$\bar{\gamma}_{\text{MCC}}(M) = M, \quad (82)$$

without regard to the distribution of γ_j or the possible dependence of these variables.

The average local power ratio for $L = [0, 2, 6, 10, 20, \dots, 100]$ is shown in Fig. 14 (b) for dual branch combining (denoted as MCC-2), triple branch combining (denoted as MCC-3) and quad branch combining (denoted as MCC-4) techniques. From this figure, it can be found that the local power ratios are 2, 3, and 4 respectively and they do not change even if L varies. This shows that for MCC, the correlation between branches has no effect on the average local power ratios.

F.2.3 Comparison of MCS/MCC and OFDM for Coded Case

To achieve the maximum channel diversity order $L + 1$, the complex-field coding is adopted for both the proposed method and OFDM. For the coded case, the data rates are K/N for MCS/MCC and $K/(N + L_{cp})$ for OFDM.

The performance can be compared by performing pairwise error probability (PEP) analysis. It is assumed that a vector \mathbf{s} is transmitted but is erroneously decoded as $\hat{\mathbf{s}} \neq \mathbf{s}$. The set of all possible error vectors is defined as

$$\mathbf{s}_e = \{\mathbf{e} = \mathbf{s} - \hat{\mathbf{s}} \mid \mathbf{s}, \hat{\mathbf{s}} \in S\}, \quad (83)$$

where S is the set of all possible vectors that \mathbf{s} may belong to. The PER is approximated using the Chernoff bound as [19]

$$P(\mathbf{s} \rightarrow \hat{\mathbf{s}} \mid \mathbf{h}) \leq \exp\left(\frac{-d^2(\mathbf{x}, \hat{\mathbf{x}})}{4N_0}\right), \quad (84)$$

where $N_0/2$ is the noise variance per real dimension, $\mathbf{x} = \beta \mathbf{D} \Theta \mathbf{s}$, $\hat{\mathbf{x}} = \beta \mathbf{D} \Theta \hat{\mathbf{s}}$ and $d(\mathbf{x}, \hat{\mathbf{x}}) = \|\mathbf{x} - \hat{\mathbf{x}}\|$ is the Euclidean distance between \mathbf{x} and $\hat{\mathbf{x}}$.

Since

$$\mathbf{u}_e = \Theta \mathbf{e} = [u_e(0), \dots, u_e(N-1)]^T, \quad (85)$$

$$\mathbf{D} = \text{diag}[H(0), \dots, H(N-1)], \quad (86)$$

the squared Euclidean distance is presented as

$$d^2(\mathbf{x}, \hat{\mathbf{x}}) = \beta^2 \|\mathbf{D} \mathbf{u}_e\|^2 = \beta^2 \sum_{i=0}^{N-1} |u_e(i)|^2 |H(i)|^2. \quad (87)$$

From (87), it can be concluded that the differences of PEPs for OFDM and MCS/MCC come from the parameter β and \mathbf{D} . In average, \mathbf{D}^{OFDM} , \mathbf{D}_1 and \mathbf{D}_2 have equal effect on the PEP. Their diagonal items are denoted as $|H^{\text{OFDM}}(i)|$, $|H_1(i)|$ and $|H_2(i)|$ respectively. $|H^{\text{MCS}}(i)|$ denotes the diagonal item for \mathbf{D}^{MCS} , and $|H^{\text{MCC}}(i)|$ denotes the diagonal item for \mathbf{D}^{MCC} . Since the selection in MCS and the combing in MCC, it is obvious that

$$\begin{aligned} |H^{\text{MCC}}(i)|^2 &\geq |H^{\text{MCS}}(i)|^2 \geq |H_1(i)|^2, \\ |H^{\text{MCC}}(i)|^2 &\geq |H^{\text{MCS}}(i)|^2 \geq |H_2(i)|^2. \end{aligned} \quad (88)$$

Therefore in average, by neglecting β , it can be obtained that

$$d^2(\mathbf{x}^{\text{MCC}}, \hat{\mathbf{x}}^{\text{MCC}}) = \sum_{i=0}^{N-1} |u_e(i)|^2 |H^{\text{MCC}}(i)|^2 \geq \sum_{i=0}^{N-1} |u_e(i)|^2 |H^{\text{MCS}}(i)|^2 = d^2(\mathbf{x}^{\text{MCS}}, \hat{\mathbf{x}}^{\text{MCS}}), \quad (89)$$

and

$$d^2(\mathbf{x}^{\text{MCS}}, \hat{\mathbf{x}}^{\text{MCS}}) \geq \sum_{i=0}^{N-1} |u_e(i)|^2 |H_1(i)|^2 \approx \sum_{i=0}^{N-1} |u_e(i)|^2 |H^{\text{OFDM}}(i)|^2 = d^2(\mathbf{x}^{\text{OFDM}}, \hat{\mathbf{x}}^{\text{OFDM}}). \quad (90)$$

In conclusion, the PEP of the proposed method is smaller than that of OFDM. By taking the power loss factors β^{MC} and β^{OFDM} into consideration, it is necessary to shift the PEP curves to the right according to the adjusted signal-to-noise ratio E_b/N_0 , where E_b is the bit energy.

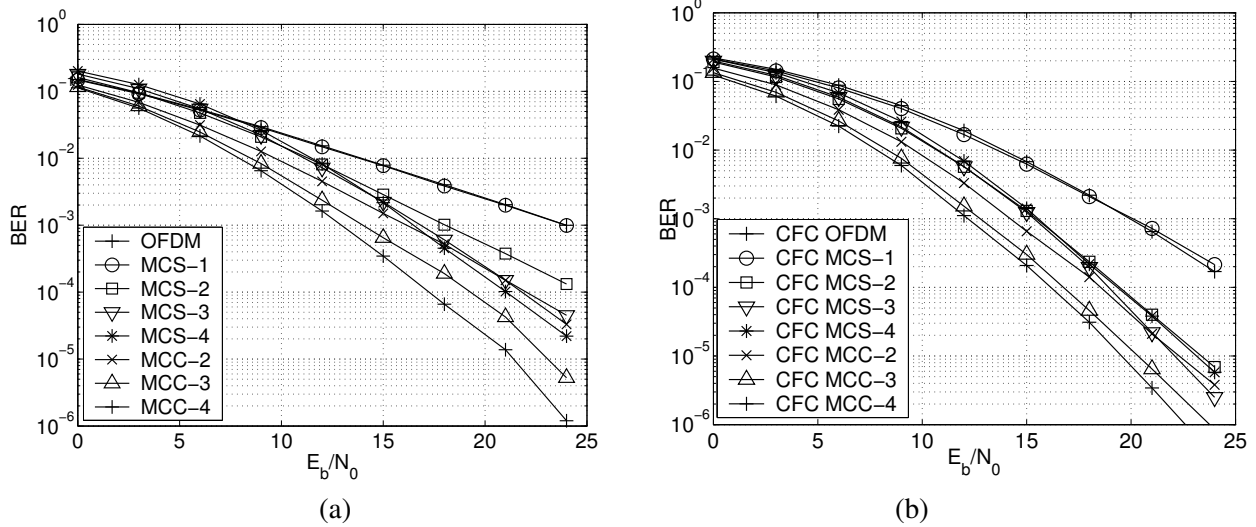


Figure 15: Performance comparison: (a) the uncoded case; (b) the case with CFC.

F.3 Simulations and Discussion

Monte-Carlo simulations are used to validate the theoretical analysis. First of all, the BERs for OFDM, MCS and MCC in the uncoded case are evaluated. MCS up to four branches are tested. These MCS schemes are denoted as MCS-1, MCS-2, MCS-3 and MCS-4 for different number of branches. MCC from two to four branches are tested. These MCC schemes are denoted as MCC-2, MCC-3 and MCC-4. The total transmission power is kept the same in all schemes. All schemes use the same frequency band. The baseband modulation is BPSK and $L = 2$.

For MCS and MCC, the frequency band is divided into $M = 1000$ subchannels and the block size is $N = 64$. In each branch of MCS or MCC, the frequency for each symbol is selected randomly from M subchannels. Then, their performance in the coded case is evaluated. The CFC coder used for all methods is the first K columns of an $N \times K$ FFT matrix, which is represented as

$$[\Theta]_{n,v} = e^{-j2\pi nv/N}$$

with $K = N - L$. Note that the transmission rate is not considered in these simulations, because the rate difference between OFDM and the proposed methods is neglectable due to a small L and a large N .

As shown in Fig. 15 (a), the performance of MCS-1 is comparable with OFDM as the previous analysis. Even with the constant total transmission power, the performance of MCS and MCC is superior than OFDM. The extra performance improvement comes from the selection and combining diversity. As shown in Fig. 15 (b), performance has been improved by using CFC. Due to the diversity techniques, MCS and MCC still outperform OFDM. It can be found that MCS-3 and MCS-4 do not improve much performance over MCS-2, and the performance of MCS-4 is even worse than that of MCS-2 for low SNR. Therefore, MCS-2 is the best choice for the tradeoff of the decreased power in each branch and the increased diversity by using multiple branches. Moreover, MCS-2 is more spectral efficient and less complex than MCS-3 and MCS-4. In addition, MCC outperforms MCS and its performance improves as the number of branches increases.

F.4 Application to the DCT Design

In this section, the selection/combining diversity technique is applied to the DCT design. The case that multiple synchronized piconets with uncoded packets coexist in frequency-selective channels is considered. Notice that here the frequency is the same for all bits in a packet. The fading is assumed to be slow so that the channel is the same for every packet, but varies from packet to packet. It is also assumed that the CSI and the hop frequencies of SCT and DCT are known to the receiver.

With SCT, a packet is successfully received only when no bit error occurs due to frequency collision, frequency-selective fading or channel noise effect. With DCT, the same packet is transmitted on two channels and they are decoded separately. A packet is successfully received if the packet on at least one channel survives.

The selection/combining diversity technique is applied in the DCT design and it is assumed that the frequency collision can be detected. Whenever there is a collision in one channel, the packet transmitted on this channel is discarded, and the packet transmitted on the uncollided channel is decoded; however, if both channels do not experience collision, the selection/combining technique is applied on the two branches at the receiver before decoding. With DCT-MCS or DCT-MCC, a packet is successfully received only in two cases: the first case is that no frequency collision happens in both channels and by using selection/combining technique, every bit is successfully decoded; the other case is that frequency collision happens in only one channel and every bit in the other channel is successfully decoded.

Let ρ denote E_b/N_0 . The PER for n synchronized piconets with SCT in frequency-selective fading channels is

$$\bar{P}_{sct}^s(k, n) = 1 - s_0^{n-1} \phi_k(\rho), \quad (91)$$

where $s_0 = (M - 1)/M$ denotes the probability that one interfering piconet chooses another frequency instead of the one chosen by the piconet of interest. $k = 1, 3, 5$ denotes the packet type. The superscript s in $\bar{P}_{sct}^s(k, n)$ indicates the synchronized case. $\phi_k(\rho)$ denotes the packet success probability for a k -slot packet in frequency-selective fading channels.

The PER of DCT for n synchronized piconets in frequency-selective fading channels is

$$\bar{P}_{dct}^s(k, n) = 1 - \sum_{i=0}^{n-1} 2^i \binom{n-1}{i} d_0^{n-1-i} d_1^{\langle i>0} (d_2^{i-1})^{\langle i>1} [1 - (1 - \phi_k(\rho/2))^2]^{\langle i=0 \rangle} \phi_k(\rho/2)^{\langle i>0} \quad (92)$$

where d_0, d_1, d_2 are defined as in Eqn. 11. $E^{\langle F \rangle}$ is equal to E if F is true, otherwise $E^{\langle F \rangle}$ is equal to 1. In (92), $\binom{n-1}{i}$ is the number of ways of selecting i unordered piconets from $n - 1$ piconets, where each selected piconets has one interfering frequency, and 2^i is the number of possible permutations of the interfering frequencies from the i piconets. $\rho/2$ reflects that the received E_b/N_0 in each of the two channels in DCT is half of what would be in SCT.

The PERs of DCT-MCS and DCT-MCC for the n synchronized piconets in frequency-selective fading channels are

$$\bar{P}_{dct-MCS}^s(k, n) = 1 - \sum_{i=0}^{n-1} 2^i \binom{n-1}{i} d_0^{n-1-i} d_1^{\langle i>0} (d_2^{i-1})^{\langle i>1} [\phi_k^{MCS}(\rho/2)]^{\langle i=0 \rangle} \phi_k(\rho/2)^{\langle i>0} \quad (93)$$

$$\bar{P}_{dct-MCC}^s(k, n) = 1 - \sum_{i=0}^{n-1} 2^i \binom{n-1}{i} d_0^{n-1-i} d_1^{\langle i>0} (d_2^{i-1})^{\langle i>1} [\phi_k^{MCC}(\rho/2)]^{\langle i=0 \rangle} \phi_k(\rho/2)^{\langle i>0} \quad (94)$$

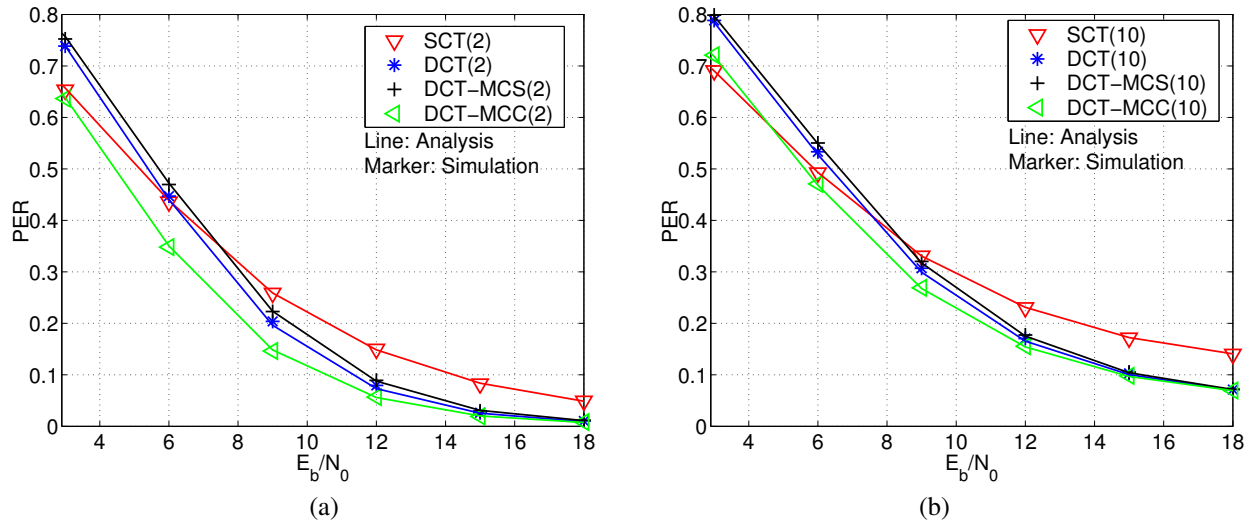


Figure 16: PER in fading channels when number of piconets is (a) 2; (b) 10.

where MCS or MCC denotes the multi-carrier selection/combining diversity technique.

The simulation results for PER of SCT, DCT, DCT-MCS and DCT-MCC with one-slot packet in frequency-selective fading channels are shown in Fig. 16 for two cases. One is for a total number of piconets of 2, the other is for a total number of piconets of 10. The modulation technique is BPSK. E_b/N_0 varies from 3 to 18 dB. From this figure, it can be found that DCT-MCS does not improve the performance of DCT. But DCT-MCC improves the performance of DCT, especially in low E_b/N_0 range. The improvement is not obvious when the total number of piconets is bigger because in this case the PER is dominated by collision. It can be found that all DCT-based methods outperform SCT when $E_b/N_0 > 8$ dB.

G Conclusions

We developed a dual transmission technique for coexistence of wireless networks. This method uses two frequency channels to deal with both dynamic and static co-channel interference. To evaluate its performance, several metrics are analyzed, including PER and throughput. Theoretic analysis and numerical simulations demonstrated that when the number of co-located piconets is less than about 20 and SNR is higher than 18 dB, the DCT design offers significant performance improvement over SCT, which makes it attractive in most practical scenarios where only a small number of piconets can possibly coexist in a physical environment due to the short transmission range of Bluetooth. With channels separated by at least 22 MHz, the DCT design is also robust to WLAN interference. This method is characterized by its independency, efficiency and robustness, requiring no interference detection, transmission delay, or traffic control. Its key limitations is the requirement for additional channel and reduced transmission range.

In addition, a multi-carrier diversity technique for single-antenna systems in frequency-selective channels is presented. By transmitting symbols on multiple frequency hopped channels, each branch of the proposed technique exhibits similar characteristic as OFDM while maintaining full data transmission rate for the uncoded case. Since symbols transmitted on different frequencies are separable, the selection/combining diversity offered by this design is explored. In the coded case, the proposed design achieves maximum channel diversity order as CFC-OFDM does. Performance analysis and numerical simulation results show that the proposed method outperforms OFDM in both the uncoded and coded cases. If combine the multi-

carrier diversity technique with DCT, the performance of DCT greatly outperforms SCT in channels with frequency-selective fading.

H Bibliography

- [1] D. J. Torrieri, "Mobile frequency-hopping CDMA systems," *IEEE Trans. Communications*, vol. 48, no. 8, pp. 1318–1327, Aug. 2000.
- [2] HomeRF Working Group, "*HomeRF Specification*," version 2.01, Jul. 2002, available at <http://www.palowireless.com/homerf/homerfspec.asp>.
- [3] Bluetooth Special Interest Group, Specification of the Bluetooth System, Version 2.0+EDR, Nov. 2004.
- [4] A. Conti, D. Dardari, G. Pasolini, and O. Andrisano, "Bluetooth and IEEE 802.11b coexistence: analytical performance evaluation in fading channels," *IEEE Journal on Selected Areas in Communications*, vol. 21, no. 2, pp. 259–269, Feb. 2003.
- [5] I. Howitt, "Bluetooth performance in the presence of 802.11b WLAN," *IEEE Trans. Vehicular Technology*, vol. 51, no. 6, pp. 1640–1651, Nov. 2002.
- [6] I. Howitt, "Mutual interference between independent Bluetooth piconets," *IEEE Trans. Vehicular Technology*, vol. 52, no. 3, pp. 708–718, May 2003.
- [7] T.-Y. Lin, Y.-K. Liu, and Y.-C. Tseng, "An improved packet collision analysis for multi-Bluetooth piconets considering frequency-hopping guard time effect," *IEEE Journal on Selected Areas in Communications*, vol. 22, pp. 2087–2094, Dec. 2004.
- [8] N. Golmie and F. Mouveaux, "Interference in the 2.4 GHz ISM band: impact on the Bluetooth access control performance," *Proc. IEEE Intl. Conf. on Communications*, vol. 8, pp. 2540–2545, Jun. 2001.
- [9] J. Dunlop and N. Amanquah, "High capacity hotspots based on bluetooth technology," *IEE Proceedings-Communications*, vol. 152, no. 5, pp. 521–527, Oct. 2005.
- [10] E. C. Arvelo, "Open-loop power control based on estimations of packet error rate in a Bluetooth radio," *Proc. Wireless Communications and Networking*, vol. 3, no. 5, pp. 1465–1469, Mar. 2003.
- [11] N. Golmie and N. Chevrollier, "Techniques to improve Bluetooth performance in interference environments," *Proc. Military Communications Conference*, vol. 1, pp. 581–585, Oct. 2001.
- [12] N. Golmie, N. Chevrollier, and O. Rebala, "Bluetooth and WLAN coexistence: challenges and solutions," *IEEE Trans. Wireless Communications*, vol. 10, no. 6, pp. 22–29, Dec. 2003.
- [13] C. F. Chiasserini and R. R. Rao, "Coexistence mechanisms for interference mitigation in the 2.4-GHz ISM band," *IEEE Trans. Wireless Communications*, vol. 2, no. 5, pp. 964–975, Sep. 2003.
- [14] C. D. M. Cordeiro, S. Abhyankar, R. Toshiwal, and D. P. Agrawal, "A novel architecture and coexistence method to provide global access to/from Bluetooth WPANs by IEEE 802.11 WLANs," *Proc. IEEE Int. Conf. on Performance, Computing, and Comm.*, pp. 23–30, Apr. 2003.
- [15] B. Zhen, Y. Kim, and K. Jang, "The analysis of coexistence mechanisms of Bluetooth," *Proc. IEEE 55th Vehicular Technology Conference*, vol. 1, pp. 419–423, May 2002.
- [16] IEEE Std. 802.15.2, "IEEE recommended practice for information technology – Part 15.2: coexistence of wireless personal area networks with other wireless devices operating in the unlicensed frequency bands," 2003, available at <http://standards.ieee.org/getieee802/802.15.html>.

- [17] A. Willig, K. Matheus, and A. Wolisz, "Wireless technology in industrial networks," *Proc. of the IEEE*, vol. 93, no. 6, pp. 1130–1151, Jun. 2005.
- [18] K. Yu-Kwong and M. C.-H. Chek, "Design and evaluation of coexistence mechanisms for Bluetooth and IEEE 802.11b systems," *Proc. IEEE Intl. Symposium on Personal, Indoor and Mobile Radio Communications*, vol. 3, pp. 1767–1771, Sep. 2004.
- [19] V. Tarokh, N. Seshadri, and A. R. Calderbank, "Space-time codes for high data rate wireless communication: performance criterion and code construction," *IEEE Trans. Information Theory*, vol. 44, pp. 744–765, Mar. 1998.
- [20] D. G. Brennan, "Linear diversity combining techniques," *Proceedings of the IEEE*, vol. 91, no. 2, pp. 331–356, Feb 2003.
- [21] E. Lindskog and A. Paulraj, "A transmit diversity scheme for channels with intersymbol interference," *Proc. IEEE International Conference on Communications*, vol. 1, pp. 307–311, Jun. 2000.
- [22] S. M. Alamouti, "A simple transmit diversity scheme for wireless communications," *IEEE Journal on Selected Areas in Communications*, vol. 16, pp. 1451–1458, Oct. 1998.
- [23] G. Kadel, "Diversity and equalization in frequency domain a robust and flexible receiver technology for broadband mobile communication systems," *Proc. IEEE 47th Vehicular Technology Conference*, vol. 2, pp. 894–898, May 1997.
- [24] J. Lansford, "MEHTA: A method for coexistence between co-located 802.11b and Bluetooth systems," IEEE 802.15-00/360r0, Nov. 2000. <http://www.ieee802.org/15/pub/TG2.html>.
- [25] R. E. Van Dyck and A. Soltanian, "IEEE 802.15.2, Clause 14.1- Collaborative co-located coexistence mechanism," *IEEE P802.15 Working Group for WPANs*, IEEE 802.15-01/364r0, Jul. 2001. <http://www.ieee802.org/15/pub/TG2-Draft.html>.
- [26] N. Golmie, "Bluetooth dynamic scheduling and interference mitigation," *ACM MONET*, vol. 9, no. 1, Feb. 2004.
- [27] A. El-Hoiydi, "Interference between Bluetooth networks—Upper bound on the packet error rate," *IEEE Communications Letters*, vol. 5, pp. 245–247, Jun. 2001.
- [28] W. P. Osborne and M. B. Luntz, "Coherent and noncoherent detection of CPFSK," *IEEE Trans. Communications*, vol. 22, pp. 1023–1036, Aug. 1974.
- [29] S. Samadian, R. Hayashi, and A. A. Abidi, "Demodulators for a zero-IF Bluetooth receiver," *IEEE Journal of Solid-state Circuits*, vol. 38, no. 8 pp. 1393–1396, Aug. 2003.
- [30] L. Lampe, M. Jain, and R. Schober, "Improved decoding for Bluetooth systems," *IEEE Trans. Comm.*, vol. 53, no. 1, pp. 1–4, Jan. 2005.
- [31] A. El-Hoiydi and J. D. Decotignie, "Soft deadline bounds for two-way transactions in Bluetooth piconets under co-channel interference," *Proc. IEEE Int. Conf. Emerging Technologies Factory Automation*, pp. 144–151, Oct. 2001.
- [32] J. C. Haartsen and S. Mattisson, "Bluetooth—a new low-power radio interface providing short-range connectivity," *Proc. of the IEEE*, vol. 88, no. 10 pp. 1651–1661, Oct. 2000.
- [33] S. Souissi and E. F. Mehofer, "Performance evaluation of a Bluetooth network in the presence of adjacent and co-channel interference," *Proc. Emerging Technologies Symposium: Broadband, Wireless Internet Access*, Apr. 2000.

- [34] F. Mazzenga, D. Cassioli, A. Detti, I. Habib, P. Loreti, and F. Vatalaro, "Performance evaluation in Bluetooth dense piconet areas," *IEEE Trans. Wireless Communications*, vol. 3, no. 6 pp. 2362–2373, Nov. 2004.
- [35] S. Zurbes, W. Stahl, K. Matheus, and J. Haartsen, "Radio network performance of Bluetooth," *Proc. IEEE International Conference on Communications*, vol. 3, pp. 1563–1567, Jun. 2000.
- [36] W. Y. Zou and Y. Wu, "COFDM: an overview," *IEEE Trans. Broadcasting*, vol. 41, no. 1, pp. 1–8, Mar. 1995.
- [37] Z. Wang and G. B. Giannakis, "Wireless multicarrier communications: where Fourier meets Shannon," *IEEE Signal Processing Magazine*, vol. 47, pp. 29–48, May 2000.
- [38] Z. Wang and G. B. Giannakis, "Complex-field coding for OFDM over fading wireless channels," *IEEE Trans. Information Theory*, vol. 49, no. 3, pp. 707–720, Mar. 2003.
- [39] C. Tepedelenlioglu, "Maximum multipath diversity with linear equalization in precoded OFDM systems" *IEEE Trans. Information Theory*, vol. 50, no. 1, pp. 232–235, Jan. 2004.
- [40] Z. Wang, X. Ma, and G. B. Giannakis, "OFDM or single-carrier block transmissions?" *IEEE Trans. Communications*, vol. 52, no. 3, pp. 380–394, Mar. 2004.
- [41] D. G. Brennan, "Linear diversity combining techniques," *Proc. of the IEEE*, vol. 91, no. 2, pp. 331–356, Feb. 2003.